Hydrodynamic Simulations of the Central Molecular Zone with a Realistic Galactic Potential

Jihye Shin (Korea Institute for Advanced Study)

Collaborators:

Sungsoo S. Kim[1], Junichi Baba[2], Takayuki Saitoh[2], Jeong-Sun Hwang[1], Kyungwon Chun[1], Shunsuke Hozumi[3]

([1]Kyung Hee University, Korea, [2]Tokyo Institute for Technology, Japan, [3]Shiga University, Japan)

Molecular gas distribution in the Milky Way

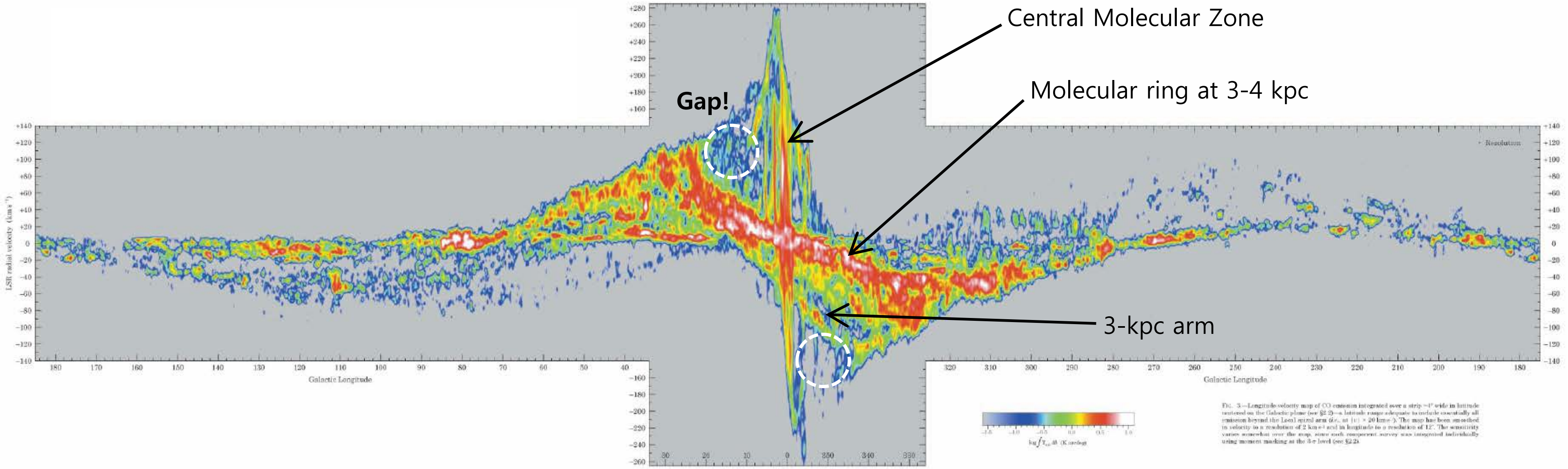

Longitude-velocity map of CO emission in -2º < b < 2º (Dame, Hartmann & Thaddeus, 2001).

Migration of gas toward the Galactic center

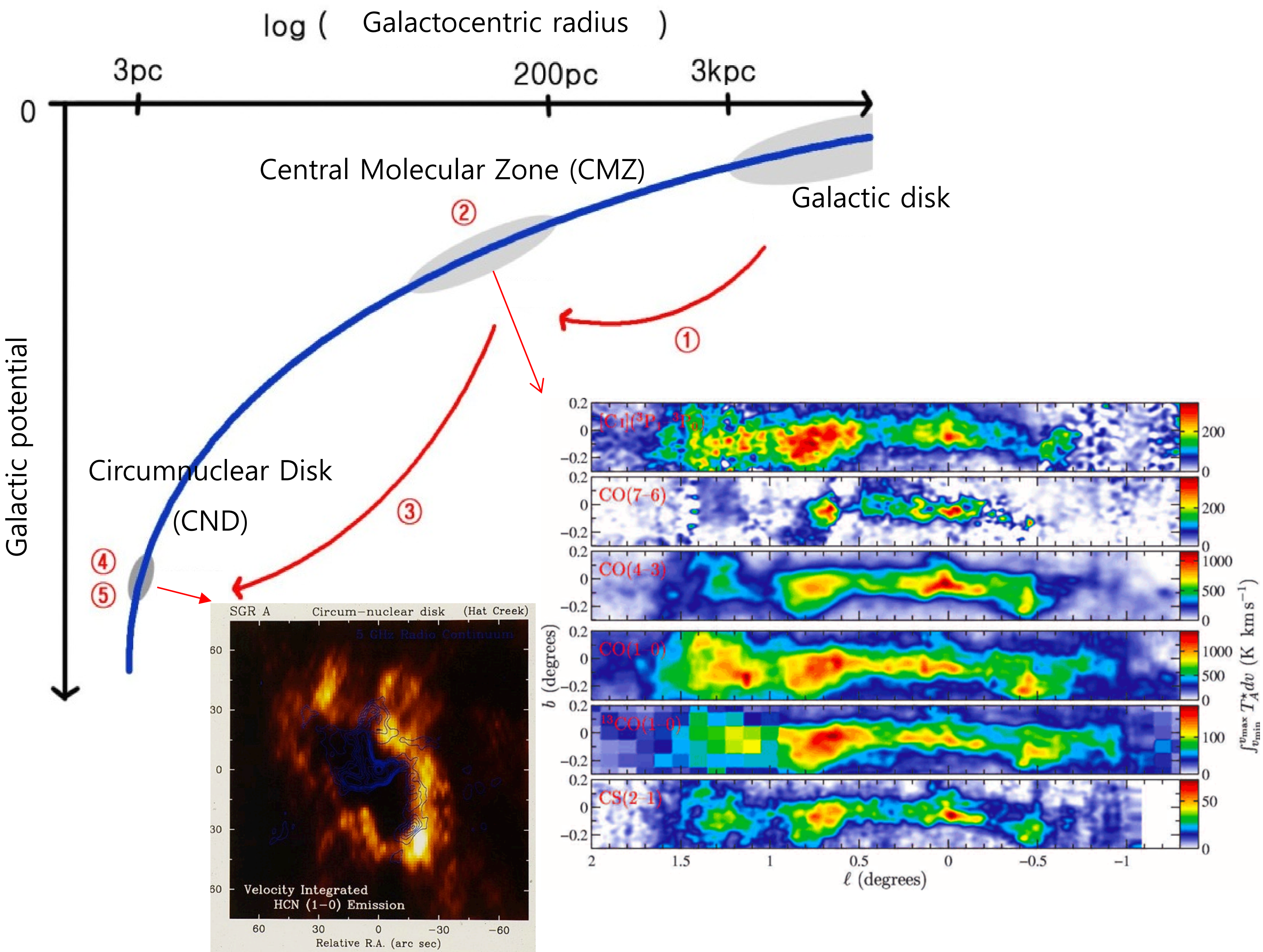

Migration of gas toward the Galactic center

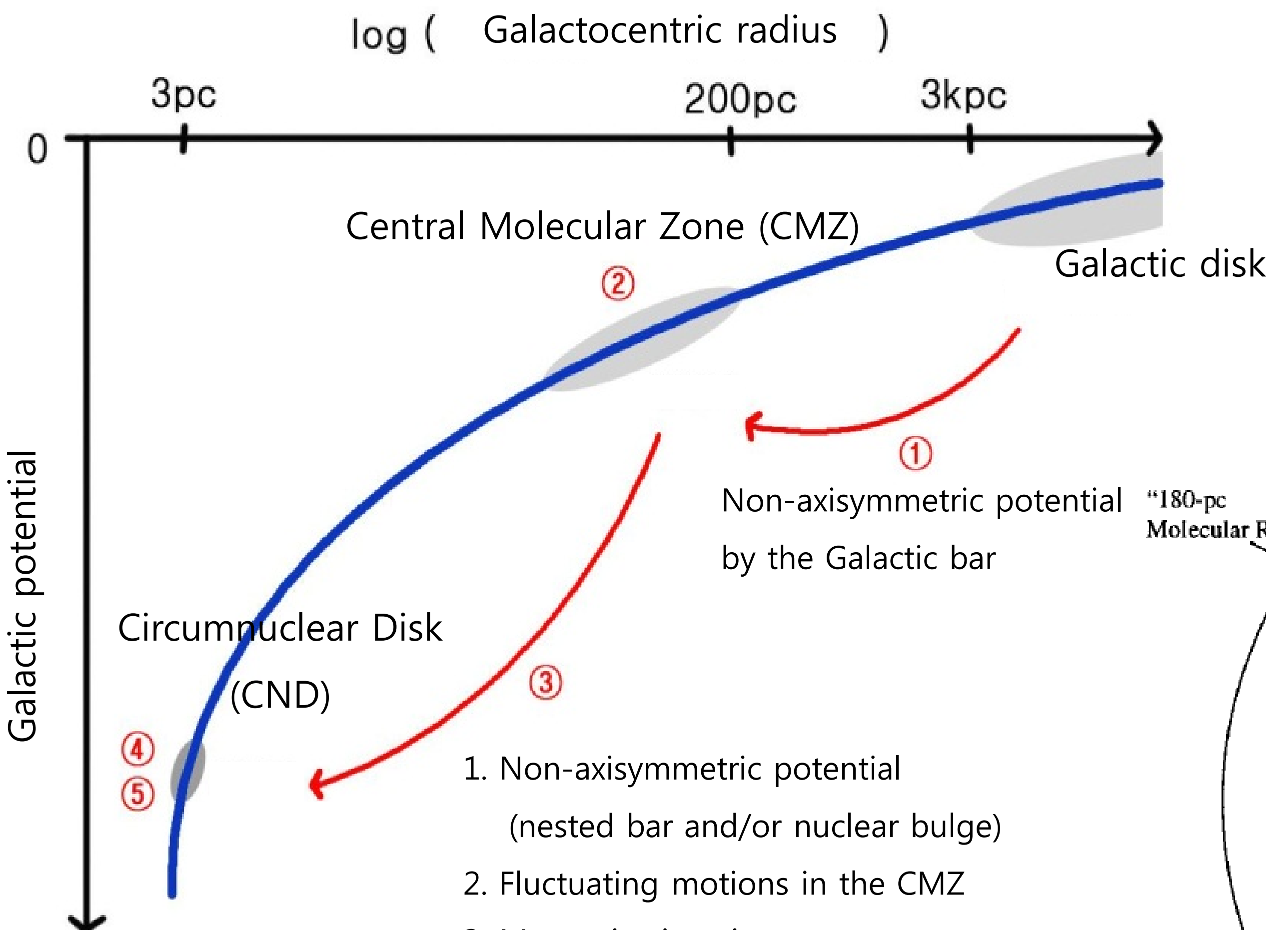

1. Non-axisymmetric potential
   (nested bar and/or nuclear bulge)
2. Fluctuating motions in the CMZ
3. Magnetic viscosity
4. Dynamical friction

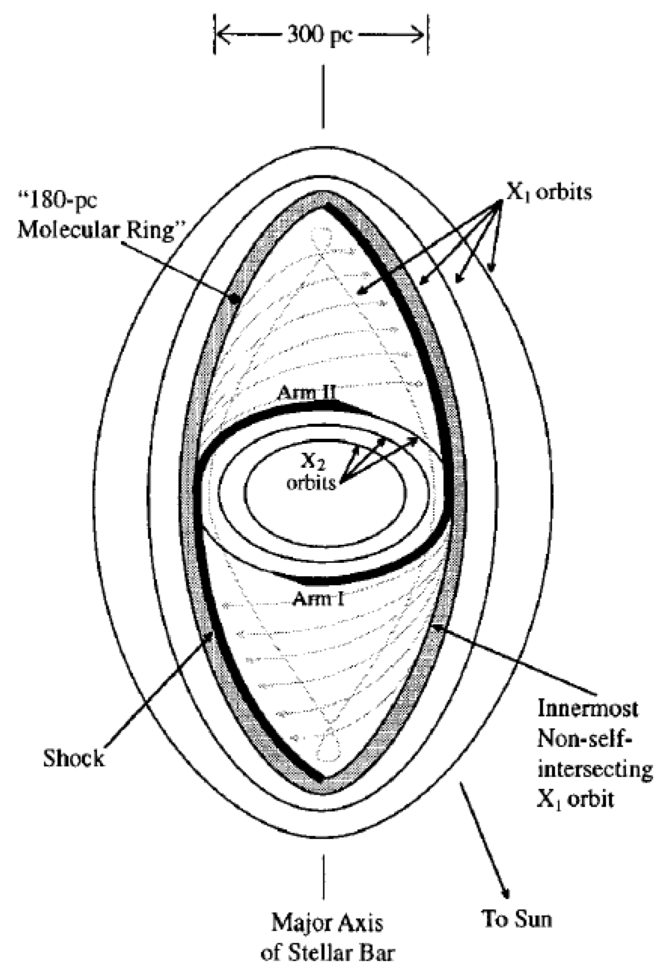

Nuclear ring in the external barred galaxies

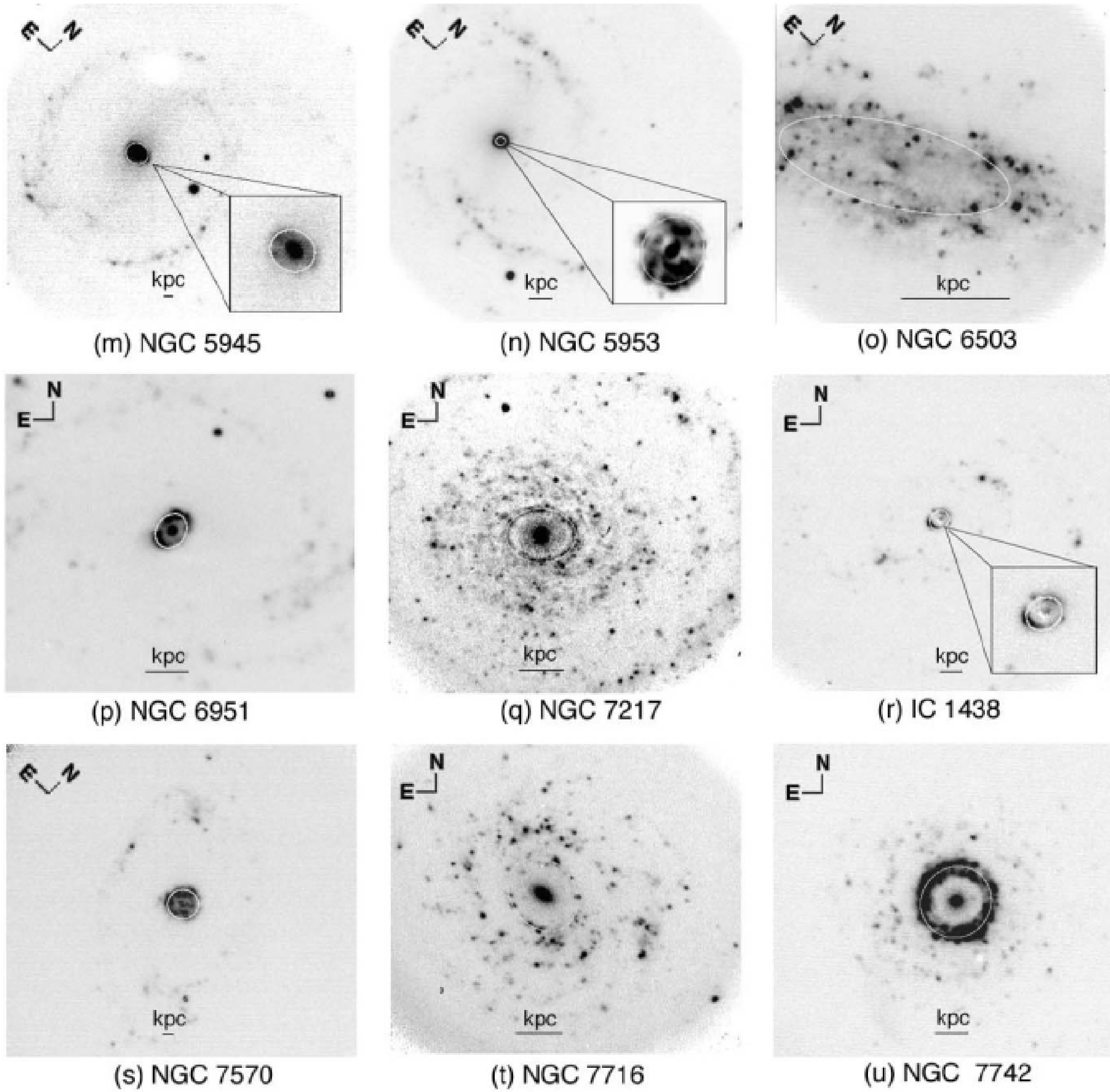

Mazzuca et al. 2008

Numerical studies

1. Jenkins & Binney (1994) with 2D sticky particle simulation

   Lee et al. (1999), Englmarier & Gerhard (1999) with 2D SPH simulation

   -> transition of gas motion from X_1 to X_2 orbits takes places in a bar potential (Binney et al. 1991)

Jenkins & Binney (1994)
2D Sticky Particle, N=8k, no self-grav

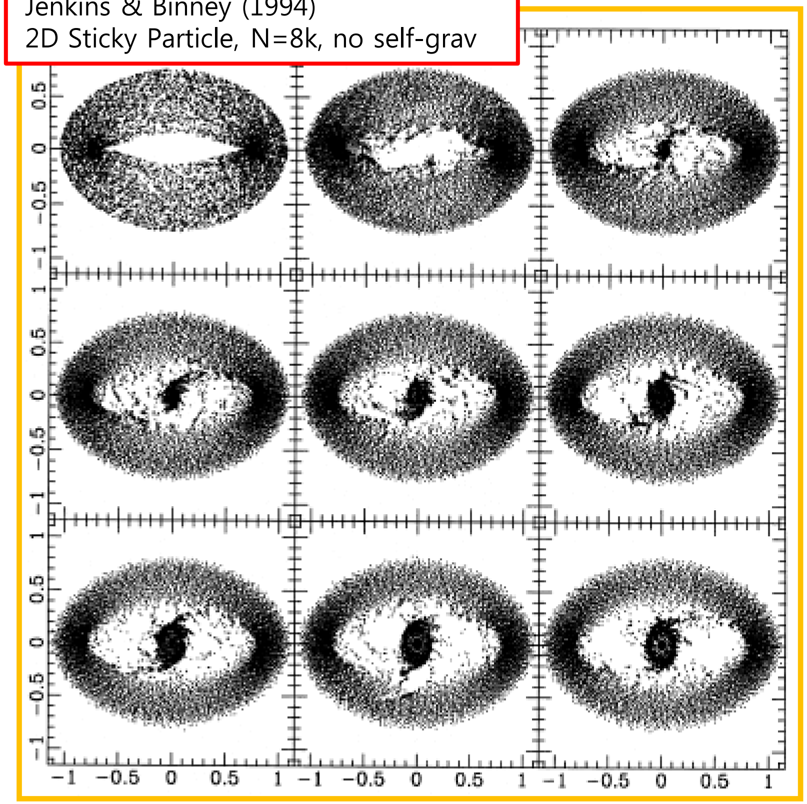

Numerical studies

1. Jenkins & Binney (1994) with 2D sticky particle simulation

   Lee et al. (1999), Englmarier & Gerhard (1999) with 2D SPH simulation

   -> transition of gas motion from X_1 to X_2 orbits takes places in a bar potential (Binney et al. 1991)

2. Rodriguez –Fernandez & Combes (2008) with 2D sticky simulation

   -> including realistic mass distribution of the Galactic bulge using 2MASS star count map

Rodriguez-Fernandez & Comes (2008)
2D hydro grid, no self-grav, N=1M

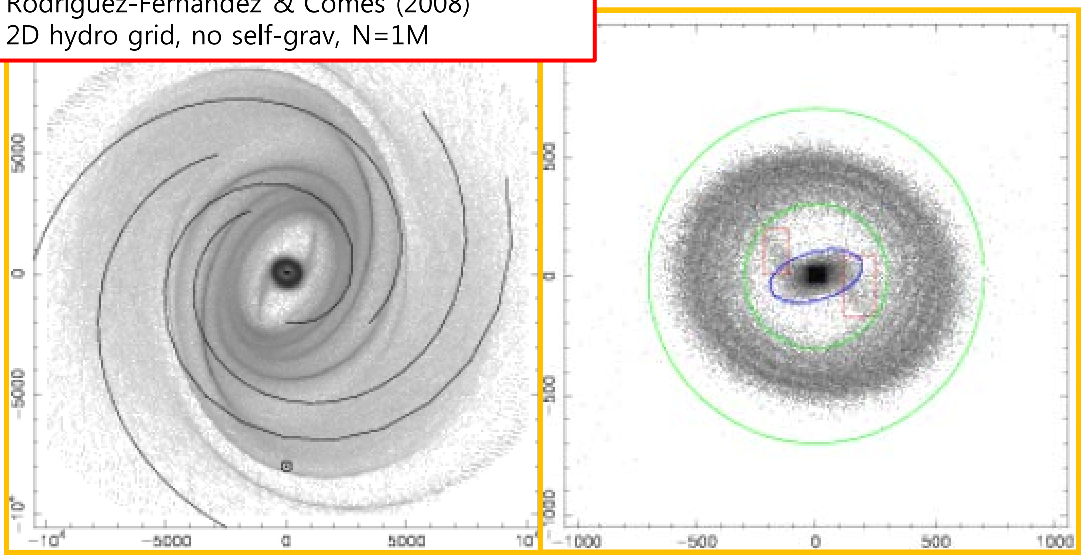

Numerical studies

1. Jenkins & Binney (1994) with 2D sticky particle simulation

   Lee et al. (1999), Englmarier & Gerhard (1999) with 2D SPH simulation

   -> transition of gas motion from X_1 to X_2 orbits takes places in a bar potential (Binney et al. 1991)

2. Rodriguez –Fernandez & Combes (2008) with 2D sticky simulation

   -> including realistic mass distribution of the Galactic bulge using 2MASS star count map

3. Kim et al. (2011) with 3D SPH simulation

   -> including realistic astrophysical processes for temperature evolution and star formation activities

Kim et al. (2011)
3D hydro particle, 3D motion, realistic astrophysical processes, self-grav, N=200K

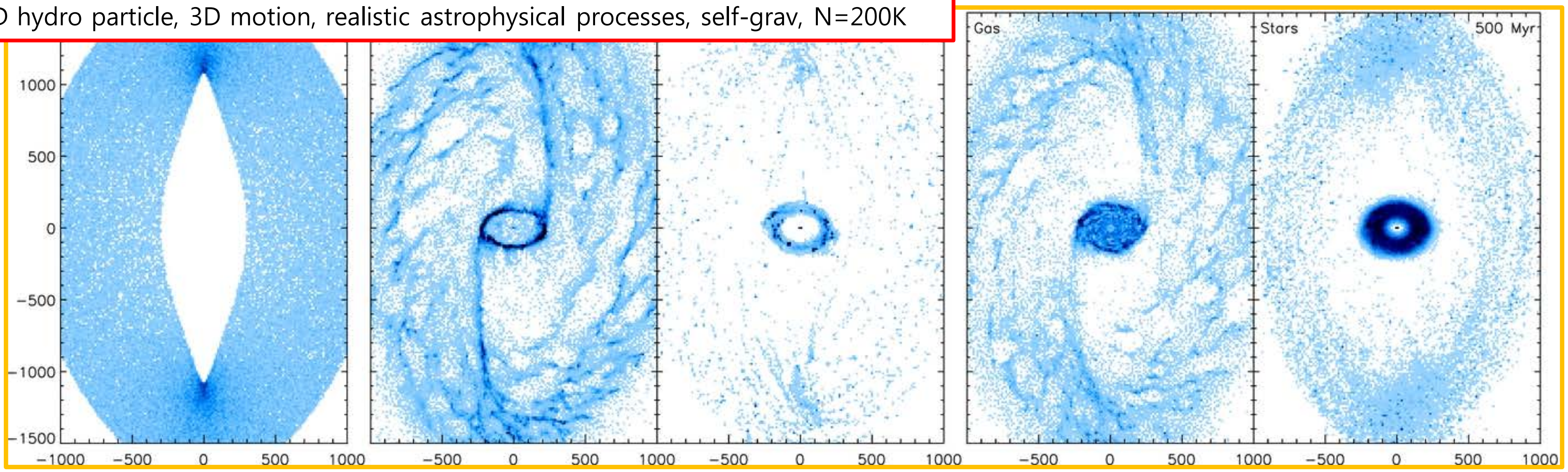

Numerical studies

1. Jenkins & Binney (1994) with 2D sticky particle simulation

   Lee et al. (1999), Englmarier & Gerhard (1999) with 2D SPH simulation

   -> transition of gas motion from X_1 to X_2 orbits takes places in a bar potential (Binney et al. 1991)

2. Rodriguez –Fernandez & Combes (2008) with 2D sticky simulation

   -> including realistic mass distribution of the Galactic bulge using 2MASS star count map

3. Kim et al. (2011) with 3D SPH simulation

   -> including realistic astrophysical processes for temperature evolution and star formation activities

4. Kim, Seo, & Kim (2012), Seo & Kim (2013, 2014) with grid-based 2D hydrodynamics

   -> physical properties and temporal evolution of nuclear ring of barred and barred-spiral galaxies

Seo & Kim et al. (2013)
2D hydro grid, self-grav, realistic astrophysical processes

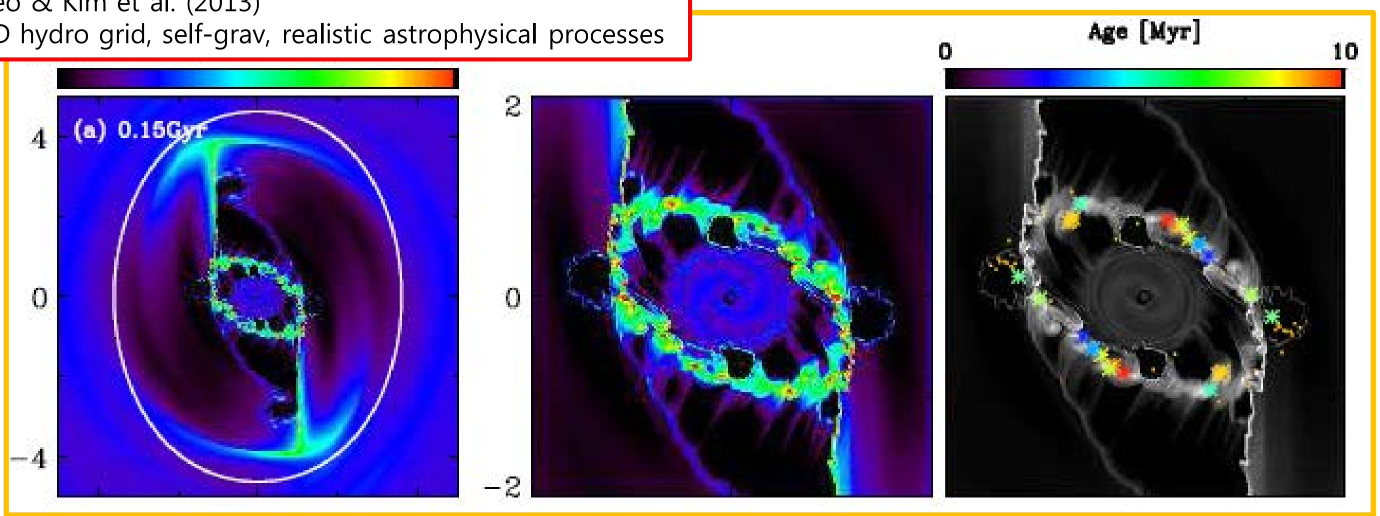

Numerical studies

1. Jenkins & Binney (1994) with 2D sticky particle simulation

   Lee et al. (1999), Englmarier & Gerhard (1999) with 2D SPH simulation

   -> transition of gas motion from X_1 to X_2 orbits takes places in a bar potential (Binney et al. 1991)

2. Rodriguez –Fernandez & Combes (2008) with 2D sticky simulation

   -> including realistic mass distribution of the Galactic bulge using 2MASS star count map

3. Kim et al. (2011) with 3D SPH simulation

   -> including realistic astrophysical processes for temperature evolution and star formation activities

4. Kim, Seo, & Kim (2012), Seo & Kim (2013, 2014) with grid-based 2D hydrodynamics

   -> physical properties and temporal evolution of nuclear ring of barred and barred-spiral galaxies

Limitations of these works

- realistic galactic potential
- various astrophysical processes in the gas
- vertical motion to the disk

In this study, we aim to trace the realistic motion of gas clouds from the Galactic disk of R_g>3 kpc to the ~200 pc CMZ under the realistic Galactic mass distribution.

The Galaxy model

The standard compound Galaxy model = bulge + disk + halo

Non-axisymmetric structure = bar + spiral arms

We adopt a simulation snapshot of Baba (2015)

that reproduces the 3D structures of the stellar disk, grand-design spiral arms, bar, and also atomic/molecular gas layers of the Milky Way.

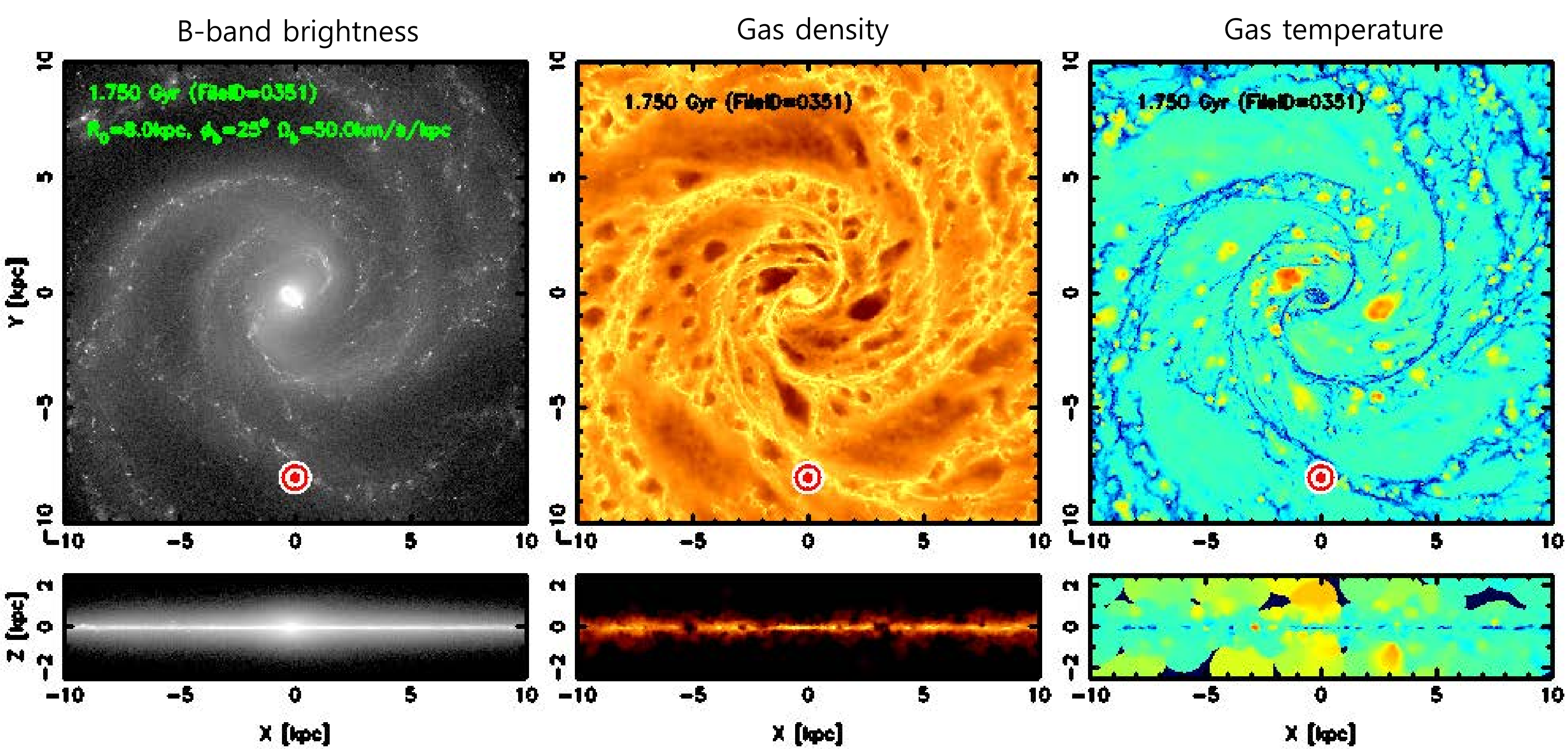

How to include the realistic 3D structures

1. Re-run the simulation?

   -> more than one month using ~1000 cores.

2. Live particles?

   -> too heavy (~10 million particles for the Galactic structures)

3. Long-range force with latticed particle distribution?

   -> fast, but not accurate

How to include the realistic 3D structures

We describe the realistic 3D structures **using multipole expansions (MEs).**

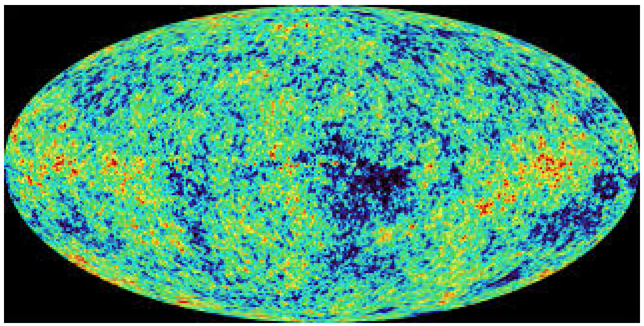

CMB (WMAP)

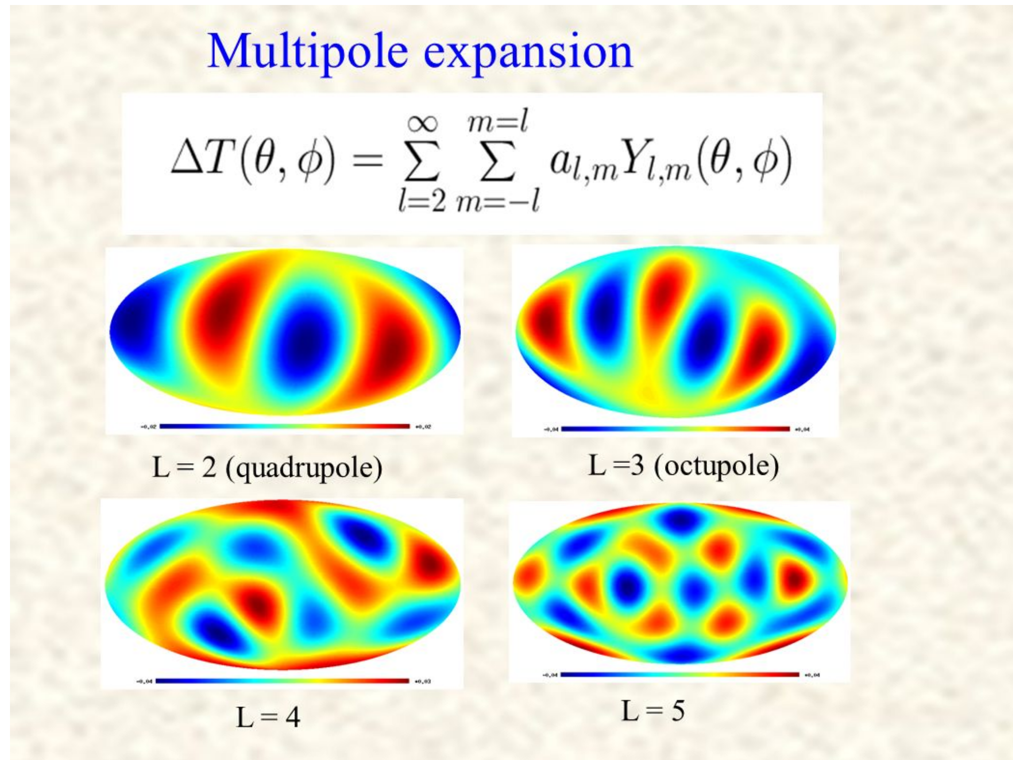

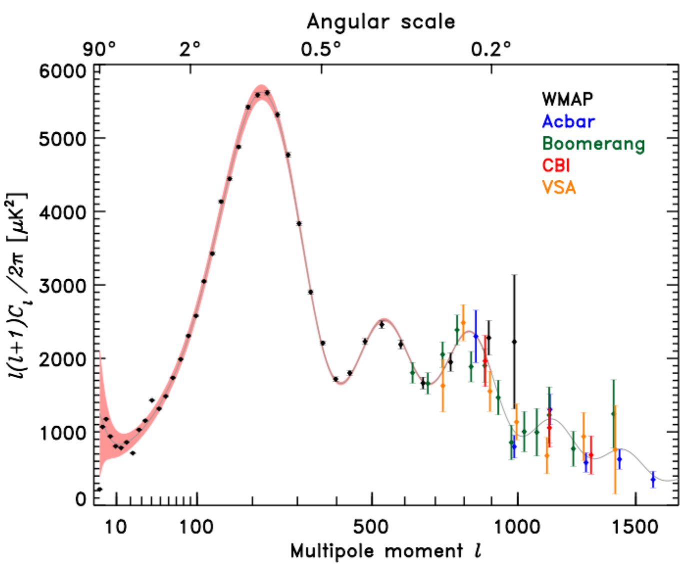

Multipole expansions to describe the Galactic structure

Bi-orthogonal basis set for density-potential pair

$$\rho(\vec{r}) = \sum_{nlm} A_{nlm} \rho_{nlm}(\vec{r}),$$

Po $$\Phi(\vec{r}) = \sum_{nlm} A_{nlm} \Phi_{nlm}(\vec{r}),$$

-> one-to-one relationship for ρ_{nlm}-Φ_{nlm}, satisfying

1. 3-dimensional, spherical model (Hernquist & Ostriker 1992) : **3D-spherical model**
2. 3-dimensional, cylindrical model (Earn 1996) : **3D-disk model**
3. 2-dimentional, polar model (Aoki & Iye 1978) : **2D-disk model**

Multipole expansions to describe the Galactic structure

1. 3-dimensional, spherical model (Hernquist & Ostriker 1992) : **3D-spherical model**

$$\rho(r,\theta,\phi) = \sum_{nlm} A_{nlm}\ \rho_{nlm}(r,\theta,\phi),$$

$$\Phi(r,\theta,\phi) = \sum_{nlm} A_{nlm}\ \Phi_{nlm}(r,\theta,\phi),$$

$$\rho_{nlm}(r,\theta,\phi) = \frac{K_{nl}}{2\pi}\frac{r^l}{r(1+r)^{2l+3}}C_n^{(2l+3/2)}\left(\frac{r-1}{r+1}\right)\sqrt{4\pi}Y_{lm}(\theta,\phi),$$

$$\Phi_{nlm}(r,\theta,\phi) = -\frac{r^l}{(1+r)^{2l+1}}C_n^{(2l+3/2)}\left(\frac{r-1}{r+1}\right)\sqrt{4\pi}Y_{lm}(\theta,\phi),$$

Gegenbauer Polynomial

Spherical harmonic

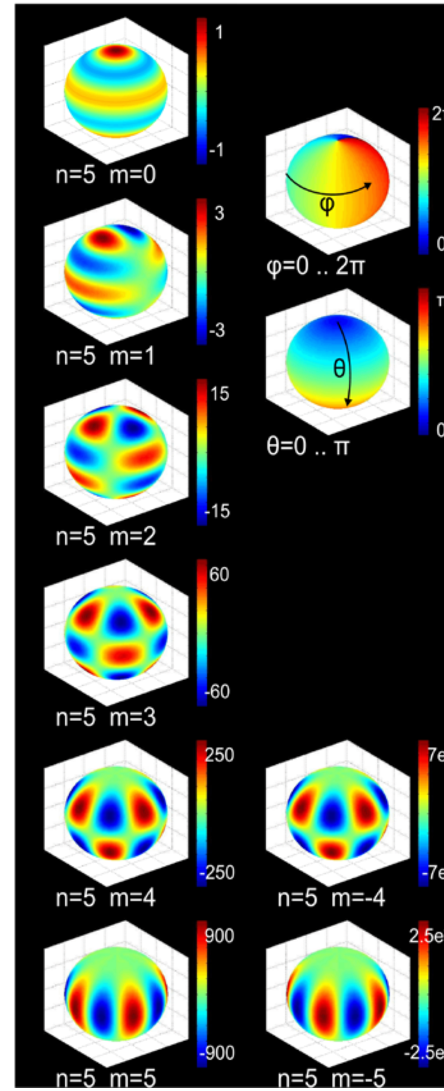

Multipole expansions to describe the Galactic structure

2. 3-dimensional, cylindrical model (Earn 1996) : **3D-disk model**

$$\rho(R,\phi,z) = \sum_{kmh} B_{kmh}\ \rho_{kmh}(r,\phi,z),$$

$$\Phi(R,\phi,z) = \sum_{kmh} B_{kmh}\ \Phi_{kmh}(r,\phi,z),$$

$$\rho_{kmh}(r,\phi,z) = \frac{1}{4\pi G} J_m(kR) e^{im\phi} k^2 e^{-k|z|},$$

$$\Phi_{kmh}(r,\phi,z) = -\frac{1}{2} J_m(kR) e^{im\phi} (1+k|z|) e^{-k|z|},$$

Cylindrical Bessel function.

3. 2-dimentional, polar model (Aoki & Iye 1978) : **2D-disk model**

$$\mu_{nm}(R,\phi) = \frac{Ma}{R_a^3} \frac{(2n+1)}{2\pi} \exp(im\phi)\ P_{nm}(r)$$

$$\Psi_{nm}(R,\phi) = -\frac{GM}{R_a} \exp(im\phi)\ P_{nm}(r)$$

Legendre function

How to use the multipole expansions

A. 3D SPHERICAL MULTIPOLE EXPANSION MODEL OF HERNQUIST & OSTRIKER (1992)

For a computational convenience, density ρ and potential Φ in a position of (r, θ, ϕ) are rewritten as

$$\rho(r,\theta,\phi) = \sum_{l=0}^{\infty}\sum_{m=0}^{l} P_{lm}(\cos\ \theta)[A_{lm}(r)\cos\ m\phi + B_{lm}(r)\sin\ m\phi],$$

$$\Phi(r,\theta,\phi) = \sum_{l=0}^{\infty}\sum_{m=0}^{l} P_{lm}(\cos\ \theta)[C_{lm}(r)\cos\ m\phi + D_{lm}(r)\sin\ m\phi],$$

where P_{lm} is a Legendre function, and A_{lm}, B_{lm}, C_{lm}, and D_{lm} are

$$\begin{bmatrix} A_{lm}(r) \\ B_{lm}(r) \\ C_{lm}(r) \\ D_{lm}(r) \end{bmatrix} = N_{lm} \sum_{n=0}^{\infty} \tilde{A}_{nl} \begin{bmatrix} \tilde{\rho}_{nl}(r) \\ \tilde{\rho}_{nl}(r) \\ \tilde{\Phi}_{nl}(r) \\ \tilde{\Phi}_{nl}(r) \end{bmatrix} \begin{bmatrix} \Sigma_{nlm}(\cos) \\ \Sigma_{nlm}(\sin) \\ \Sigma_{nlm}(\cos) \\ \Sigma_{nlm}(\sin) \end{bmatrix}.$$

Here, N_{lm}, $\tilde{A}_{nl}$, $\tilde{\rho}_{nl}$, and $\tilde{\Phi}_{nl}$ are

$$N_{lm} = \frac{2l+1}{4\pi}(2-\delta_{m0})\frac{(l-m)!}{(l+m)!},$$

$$\tilde{A}_{nl} = -\frac{2^{8l+6}}{K_{nl}\ 4\pi}\frac{n!\ (n+2l+3/2)[\Gamma(2l+3/2)]^2}{\Gamma(n+4l+3)},$$

$$\tilde{\rho}_{nl} = \frac{K_{nl}}{2\pi}\frac{r^l}{r(1+r)^{2l+3}} C_n^{(2l+3/2)}\left(\frac{r-1}{r+1}\right)\sqrt{4\pi},$$

$$\tilde{\Phi}_{nl} = -\frac{r^l}{(1+r)^{2l+1}} C_n^{(2l+3/2)}\left(\frac{r-1}{r+1}\right)\sqrt{4\pi},$$

where C_n^{α} is a Gegenbauer polynomial, and K_{nl} is a normalization constant of

$$K_{nl} = n(n+4l+3)/2 + (l+1)(2l+1).$$

Multipole expansions to describe the Galactic structure

The expansion coefficients of $\Sigma_{nlm}(\cos)$ and $\Sigma_{nlm}(\sin)$ are calculated with a collection of kth particles by

$$\begin{bmatrix} \Sigma_{nlm}(\cos) \\ \Sigma_{nlm}(\sin) \end{bmatrix} = \sum_k m_k \widetilde{\Phi}_{nl}(r_k) P_{lm}(\cos\ \theta_k) \begin{bmatrix} \cos\ m\phi_k \\ \sin\ m\phi_k \end{bmatrix}.$$

-> making tables of Σ_{nlm}(cos) and Σ_{nlm}(sin)

-> reading the tables when a simulation run starts

Similar to ρ and Φ, accelerations a_r, a_θ, and a_ϕ are derived by

$$a_r(r,\theta,\phi) = -\sum_{l=0}^{\infty}\sum_{m=0}^{l} P_{lm}(\cos\ \theta)[E_{lm}(r)\cos\ m\phi + F_{lm}(r)\sin\ m\phi],$$

$$a_\theta(r,\theta,\phi) = -\frac{1}{r}\sum_{l=0}^{\infty}\sum_{m=0}^{l} \frac{dP_{lm}(\cos\ \theta)}{d\theta}[C_{lm}(r)\cos\ m\phi + D_{lm}(r)\sin\ m\phi],$$

$$a_\phi(r,\theta,\phi) = -\frac{1}{r}\sum_{l=0}^{\infty}\sum_{m=0}^{l} \frac{mP_{lm}(\cos\ \theta)}{\sin\ \theta}[D_{lm}(r)\cos\ m\phi - C_{lm}(r)\sin\ m\phi],$$

where E_{lm} and F_{lm} are

$$\begin{bmatrix} E_{lm}(r) \\ F_{lm}(r) \end{bmatrix} = N_{lm}\sum_{n=0}^{\infty} \widetilde{A}_{nl}\frac{d}{dr}\widetilde{\Phi}_{nl}(r) \begin{bmatrix} \Sigma_{nlm}(\cos) \\ \Sigma_{nlm}(\sin) \end{bmatrix}.$$

1. 3D-disk model of Earn (1996)

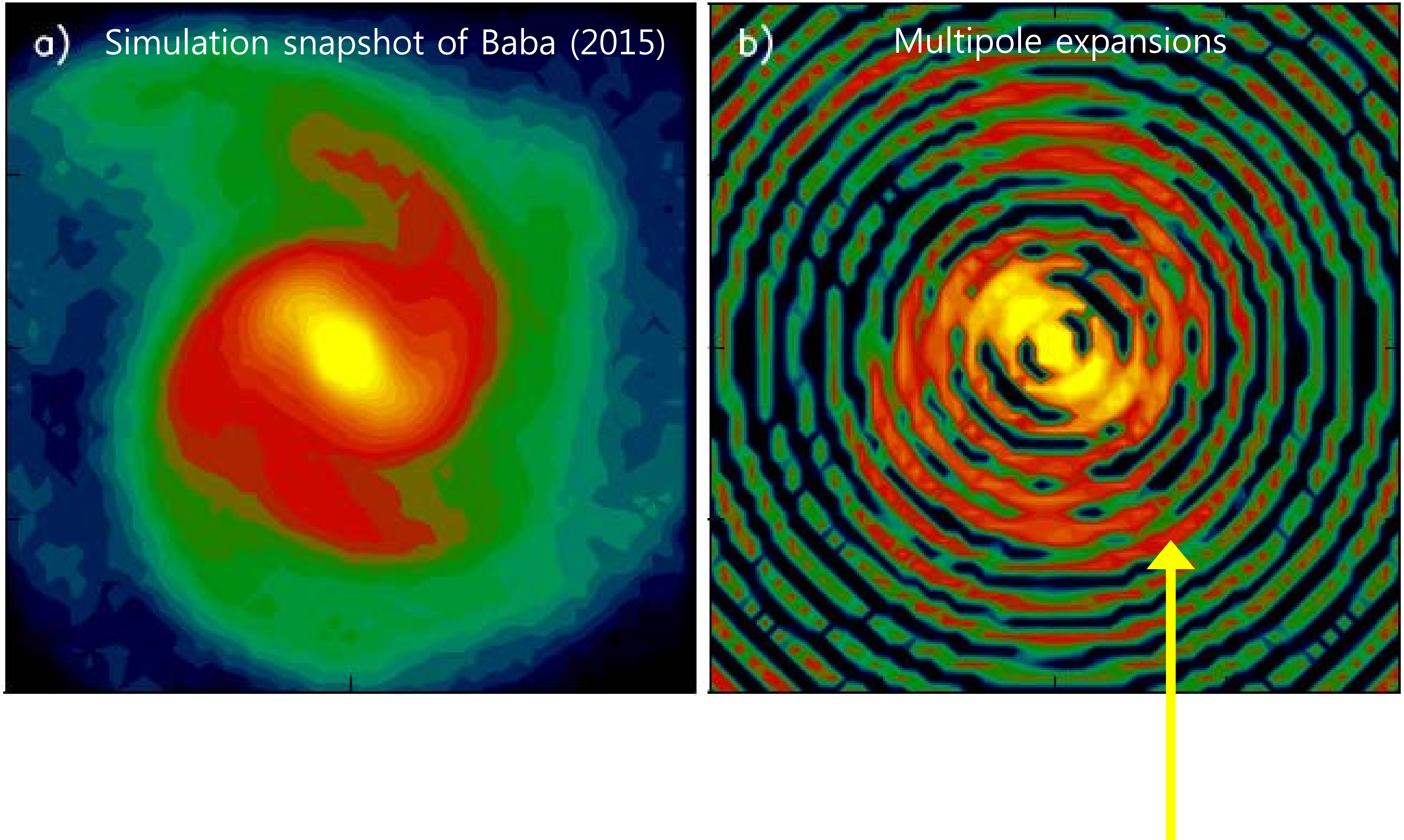

Radial density fluctuation

<Projected stellar density distribution>

Decomposition of stellar particle

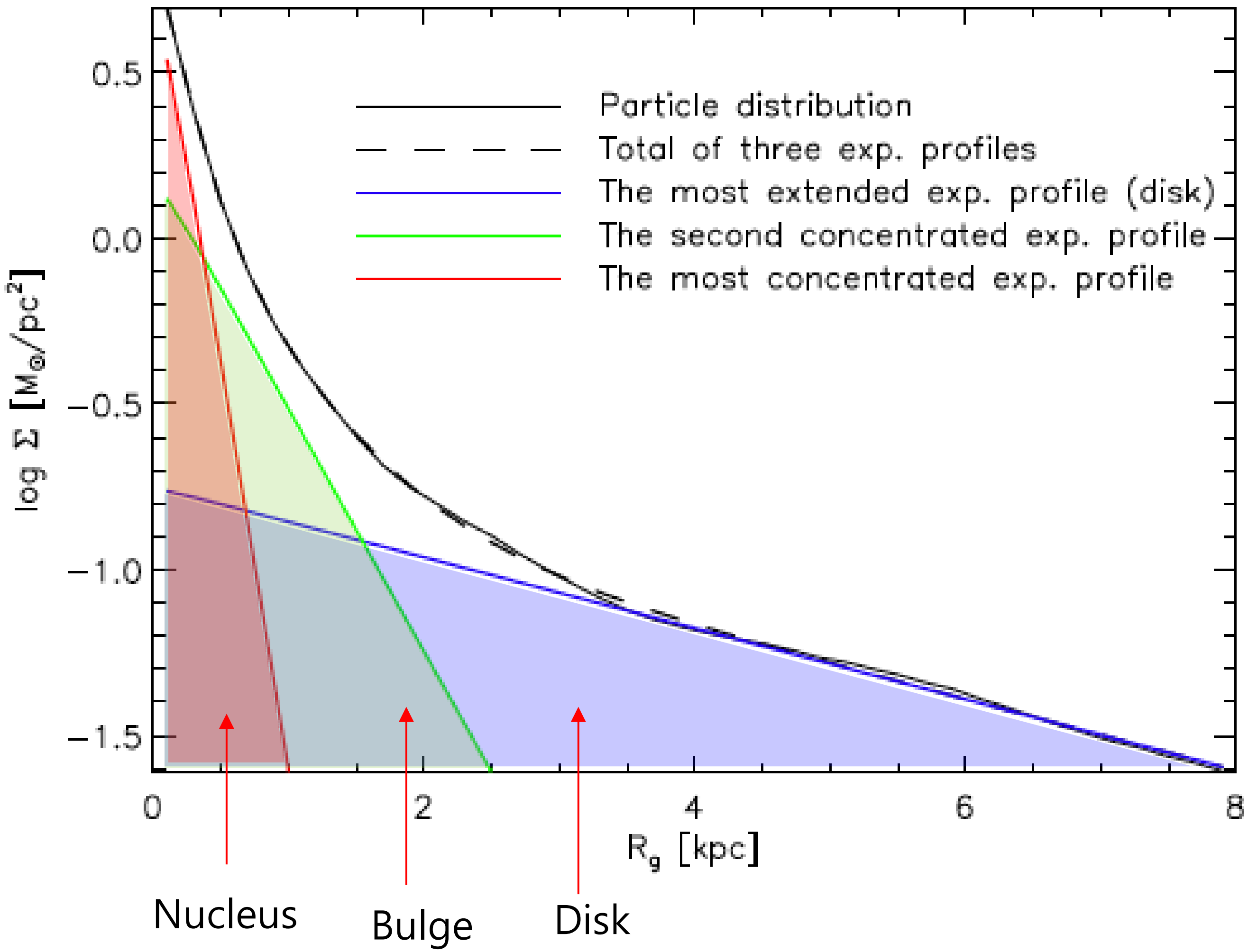

$$\rho(R_g, z) = \Sigma_0 \exp(-R_g/R_d)[\exp(-|z|/h_z)/(2h_z)]$$

2. Hybrid models (3D-spherical + 3D-disk)

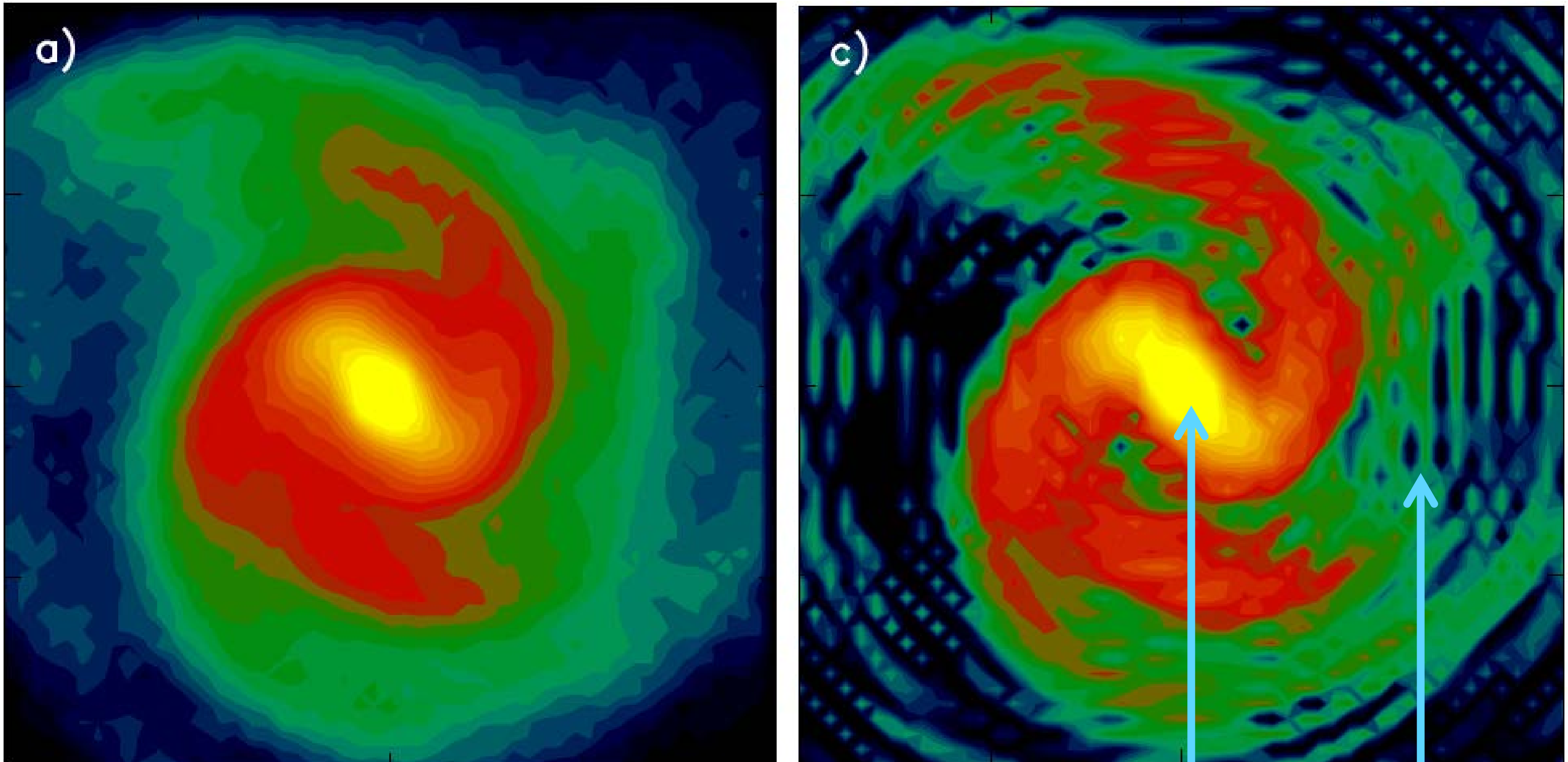

Nucleus+Bulge components : 3D-spherical model of Hernquist & Ostiker (1992)

Disk component : 3D-disk model of Earn (1996)

Bulge

Disk

<Projected stellar density distribution>

3. Hybrid models (3D-spherical + 2D-disk)

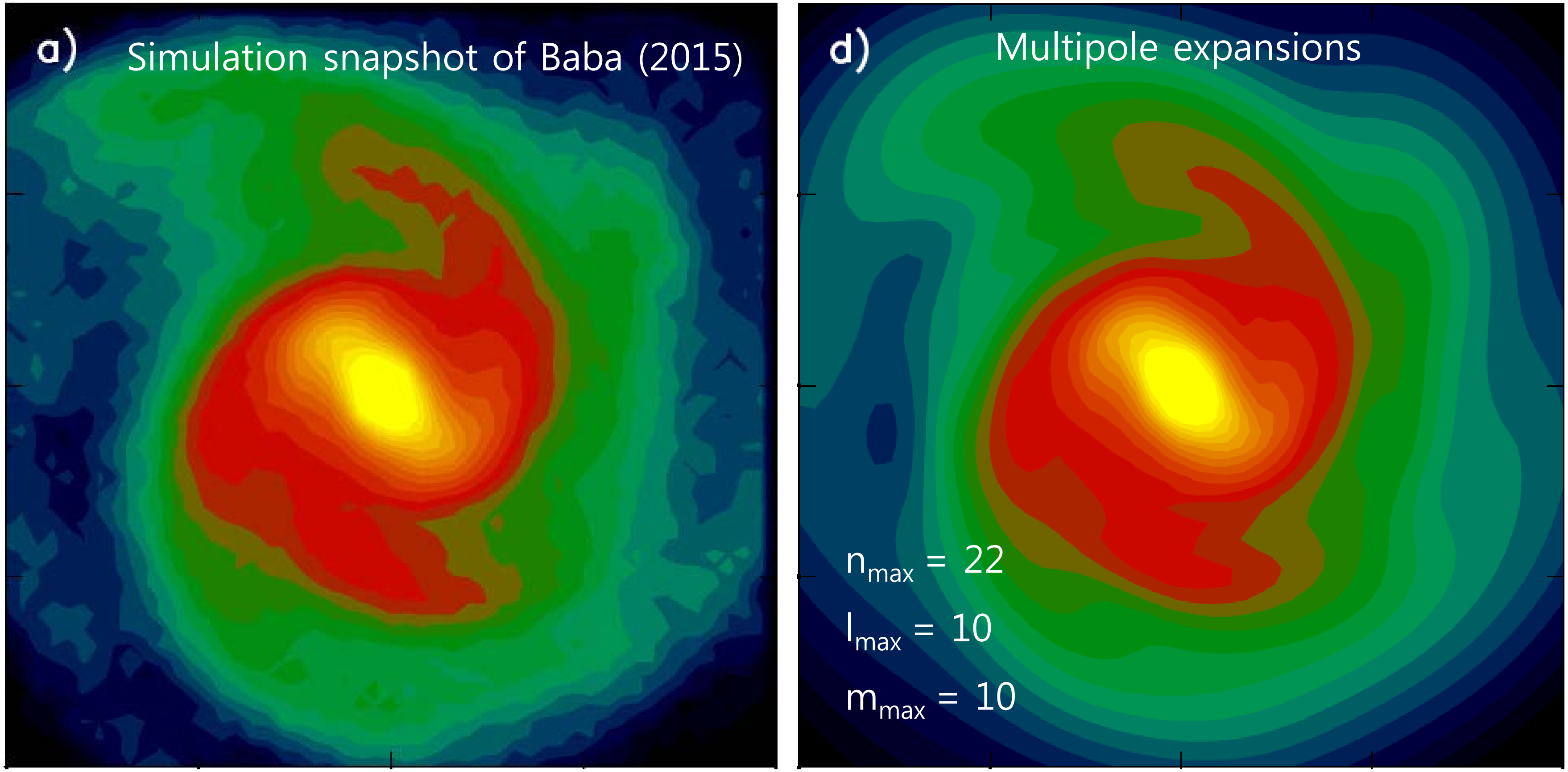

Nucleus+Bulge components : 3D-spherical model of Hernquist & Ostiker (1992)

Disk component : 2D-disk model of Aoki & Iye (1978)

<Projected stellar density distribution>

Thick disk correction (Binney & Tremaine 2008)

To overcome a limitation of the 2D-disk model…

3D disk

For a thick disk whose density profiles following

$$\rho(R_g, z) = \Sigma_0 \exp(-R_g/R_d)[\exp(-|z|/h_z)/(2h_z)],$$

Potential at a position (R_g, z) can be derived as

$$\Phi(R, z) = -\frac{4G\Sigma_0}{R_d} \int_{-\infty}^{\infty} dz' \frac{\exp(z'/h_z)}{2h_z} \int_0^{\infty} da \ \sin^{-1}\left(\frac{2a}{\sqrt{+} + \sqrt{-}}\right) aK_0(a/R_d)$$

2D disk

For an instantaneously thin disk whose density profile following

$$\Sigma(R) = \Sigma_0 \exp(-R/R_d),$$

Potential at a position (Rg, 0) can be derived as

Modified Bessel functions

$$\Phi(R, 0) = -\pi G \Sigma_0 R \left[I_0(y)K_1(y) - I_1(y)K_0(y)\right],$$

Thick disk correction (Binney & Tremaine 2008)

Difference of a_R between the 2D and 3D exponential disks :

$$\begin{aligned}\triangle a_R(R,z) &= a_R(R,z) - a_{R,0}(R) \\ &= -d\Phi(R,z)/dR + d\Phi_0(R)/dR\end{aligned}$$

a_z due to the non-zero disk thickness :

$$a_z(R,z) = -d\Phi(R,z)/dz$$

Δa_R and a_z : equally for $\phi = 0 - 2\pi$

Averaged acceleration profiles

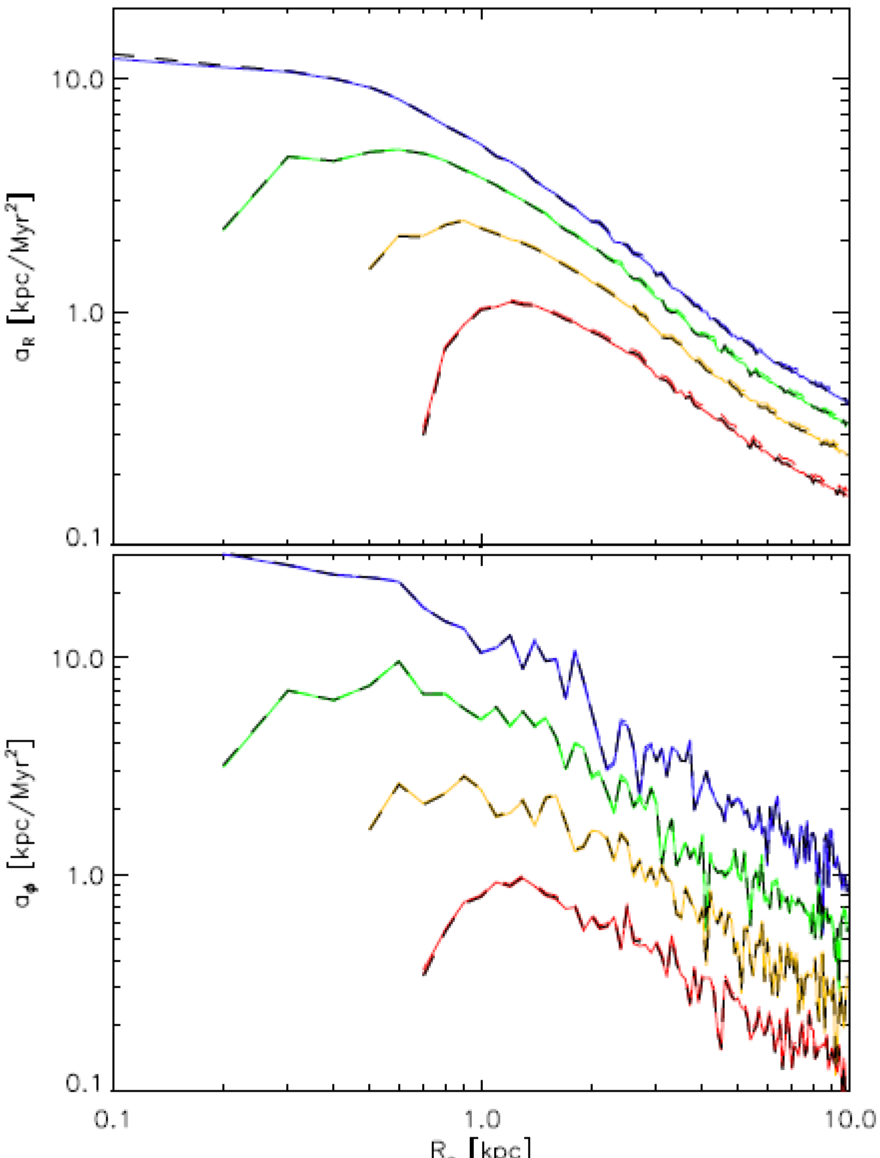

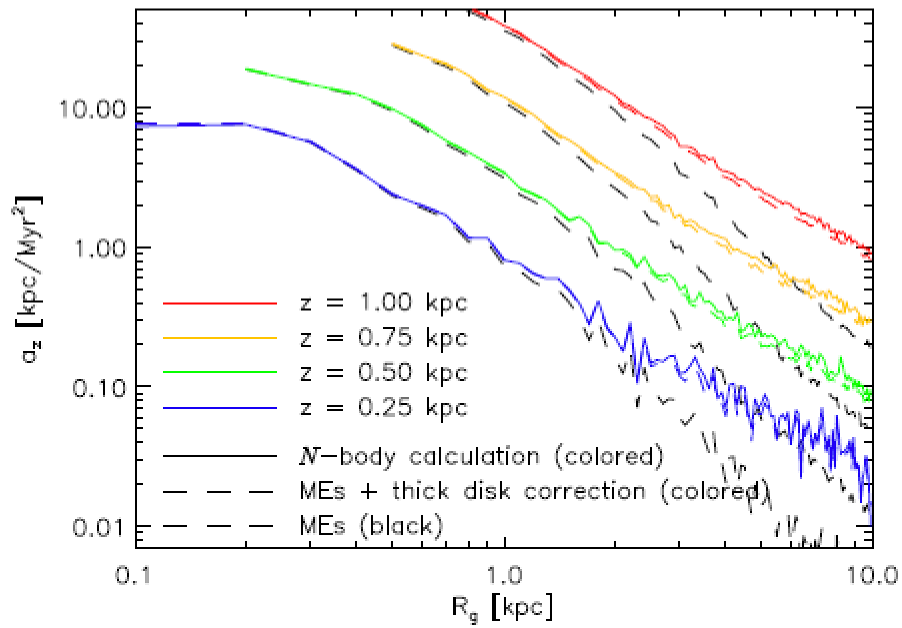

The Galactic structures are well reproduced by **2D ME + 3D ME + thick disk correction**.

Advantages of the ME method

1. We can describe the realistic mass distribution of the Milky Way.
2. Performance : ~30 times faster than 10 million live particles
3. We can enlarge/diminish a bar elongation by modifying ME coefficients (even modes).

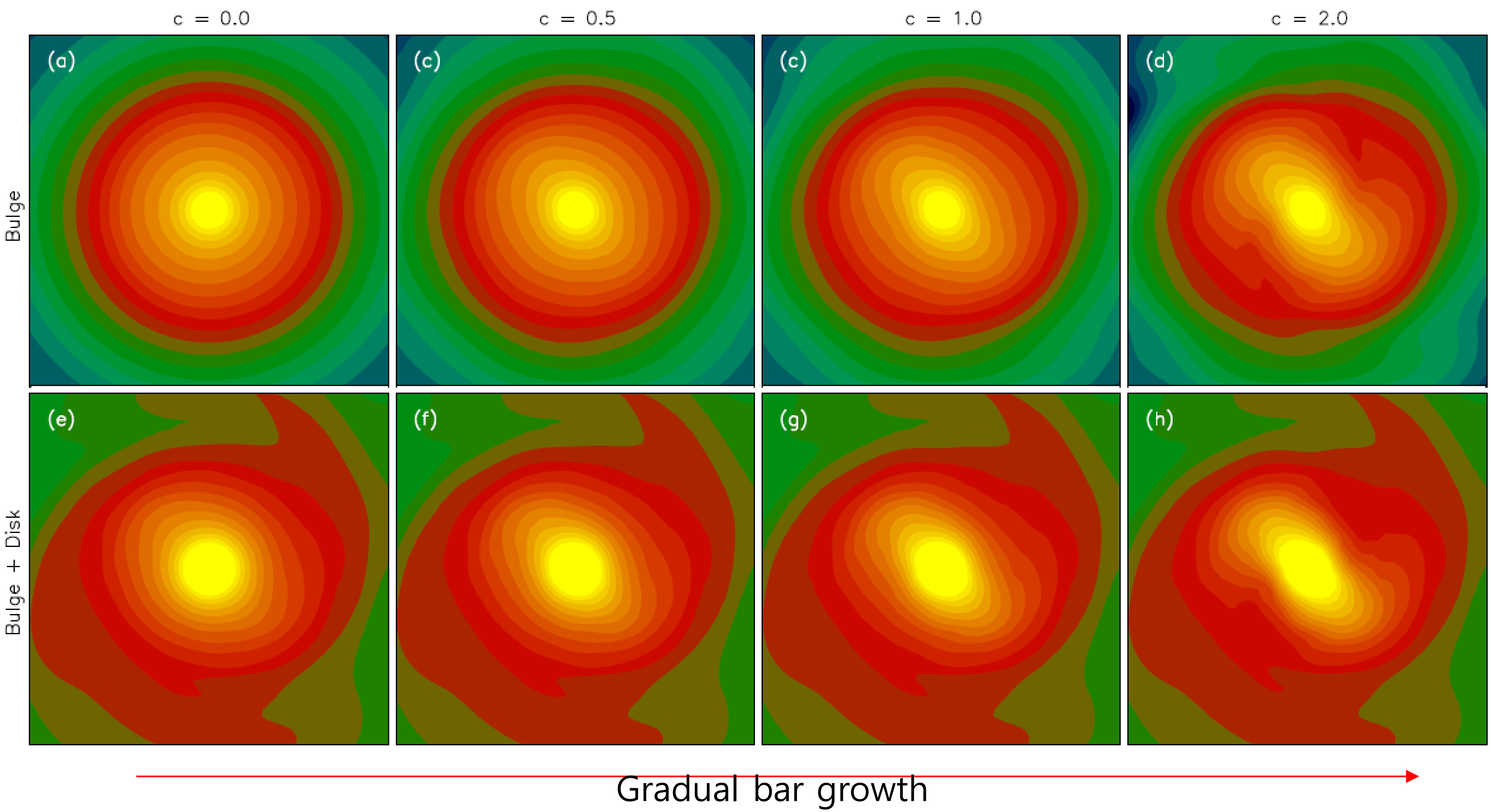

Simulation code

Simulation code : based on a parallel N-body/SPH code, **Gadget-2** (Springel 2005)

- Radiative Heating & Cooling by Cloudy 90 package (Ferland et al. 1998)

  : ionizing photon flux = 1, 100 G0 (Habing field)
- Star formation at high density (n_H > 100 cm^{-3}) and low temperature (T < 100K)
- SN II feedback (time-step limiter of Durier & Dallar Vecchia 2012, Saitoh & Makino 2009)
- High performing time-stepping (Saitoh & Makino 2010)
- Realistic Galactic potential using multipole expansions

  1. tabulating ME coefficients before a simulation
  2. Reading the ME tables when a simulation starts
  3. Calculating external force for a given particle position

- Initial particles : only for gas

Simulation parameters

MODEL PARAMETERS

Model	N_{gas}	$R_{IB} - R_{OB}$ [kpc]	Q	τ_{growth} [Myr]	Ω_{bar} [km/s/kpc]
A	10^5	0 - 6	0.284	0	35
Aq1	10^5	0 - 6	0.252	350	35
Aq2	10^5	0 - 6	0.268	350	35
Aq3	10^5	0 - 6	0.299	350	35
Aq4	10^5	0 - 6	0.315	350	35
At1	10^5	0 - 6	0.284	175	35
At2	10^5	0 - 6	0.284	350	35
At3	10^5	0 - 6	0.284	700	35
Ap1	10^5	0 - 6	0.284	350	30
Ap2	10^5	0 - 6	0.284	350	40
B	10^5	1 - 6	0.284	0	35
Bq1	10^5	1 - 6	0.252	350	35
Bq2	10^5	1 - 6	0.268	350	35
Bq3	10^5	1 - 6	0.299	350	35
Bq4	10^5	1 - 6	0.315	350	35
Bt1	10^5	1 - 6	0.284	175	35
Bt2	10^5	1 - 6	0.284	350	35
Bt3	10^5	1 - 6	0.284	700	35
Bp1	10^5	1 - 6	0.284	350	30
Bp2	10^5	1 - 6	0.284	350	40
Ah	3×10^5	0 - 6	0.284	0	35
At2h	3×10^5	0 - 6	0.252	350	35
Bh	3×10^5	1 - 6	0.284	0	35
Bt2h	3×10^5	1 - 6	0.252	350	35

Initial gas distribution : R_{IB} - R_{OB}

- Type 'A' = 0 – 6 kpc,
- Type 'B' = 1 – 6 kpc

Total number of gas particles :

normal : 10^5

high resolution : 3×10^5 (Ah, At2h,Bh,Bt2h)

Individual gas mass :

normal : $7.5\text{-}8.4 \times 10^3\ M_{sun}$

high : $2.5\text{-}2.8 \times 10^3\ M_{sun}$

Bar growth timescale (τ_{growth}) :

0, 175, 350, 700 Myr (A, At1, At2, At3)

Pattern speed (Ω_{bar}) :

30, 35, 40 km/s/kpc (Ap1, A, Ap2)

Bar strength (Q) :

0.252, 0.268, 0.284, 0.299, 0.31 (Aq1,Aq2,A, Aq3,Aq4)

Simulation parameters

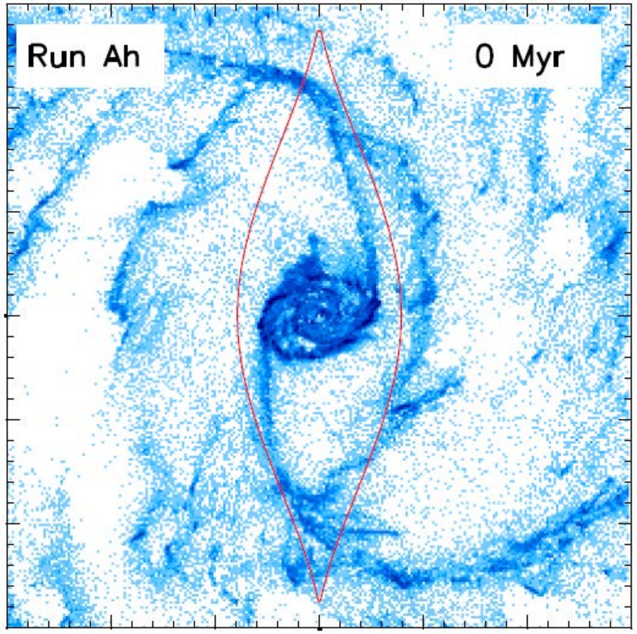

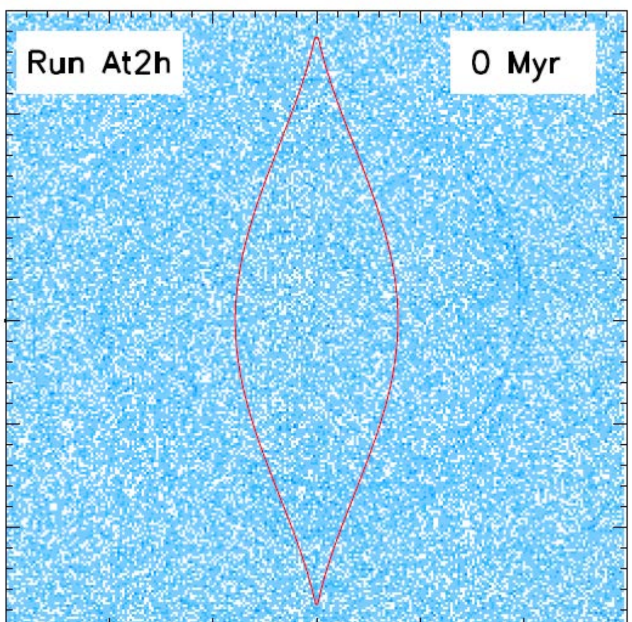

Initial gas distribution : R_{IB} - R_{OB}

- Type 'A' = 0 – 6 kpc,
- Type 'B' = 1 – 6 kpc

Total number of gas particles :

normal : 10^5

high resolution : 3×10^5 (Ah, At2h,Bh,Bt2h)

Individual gas mass :

normal : 7.5-8.4 x 10^3 M_{sun}

high : 2.5-2.8 x 10^3 M_{sun}

Bar growth timescale (τ_{growth}) :

0, 175, 350, 700 Myr (A, At1, At2, At3)

Pattern speed (Ω_{bar}) :

30, 35, 40 km/s/kpc (Ap1, A, Ap2)

Bar strength (Q) :

0.252, 0.268, 0.284, 0.299, 0.31 (Aq1,Aq2,A, Aq3,Aq4)

Overall morphology

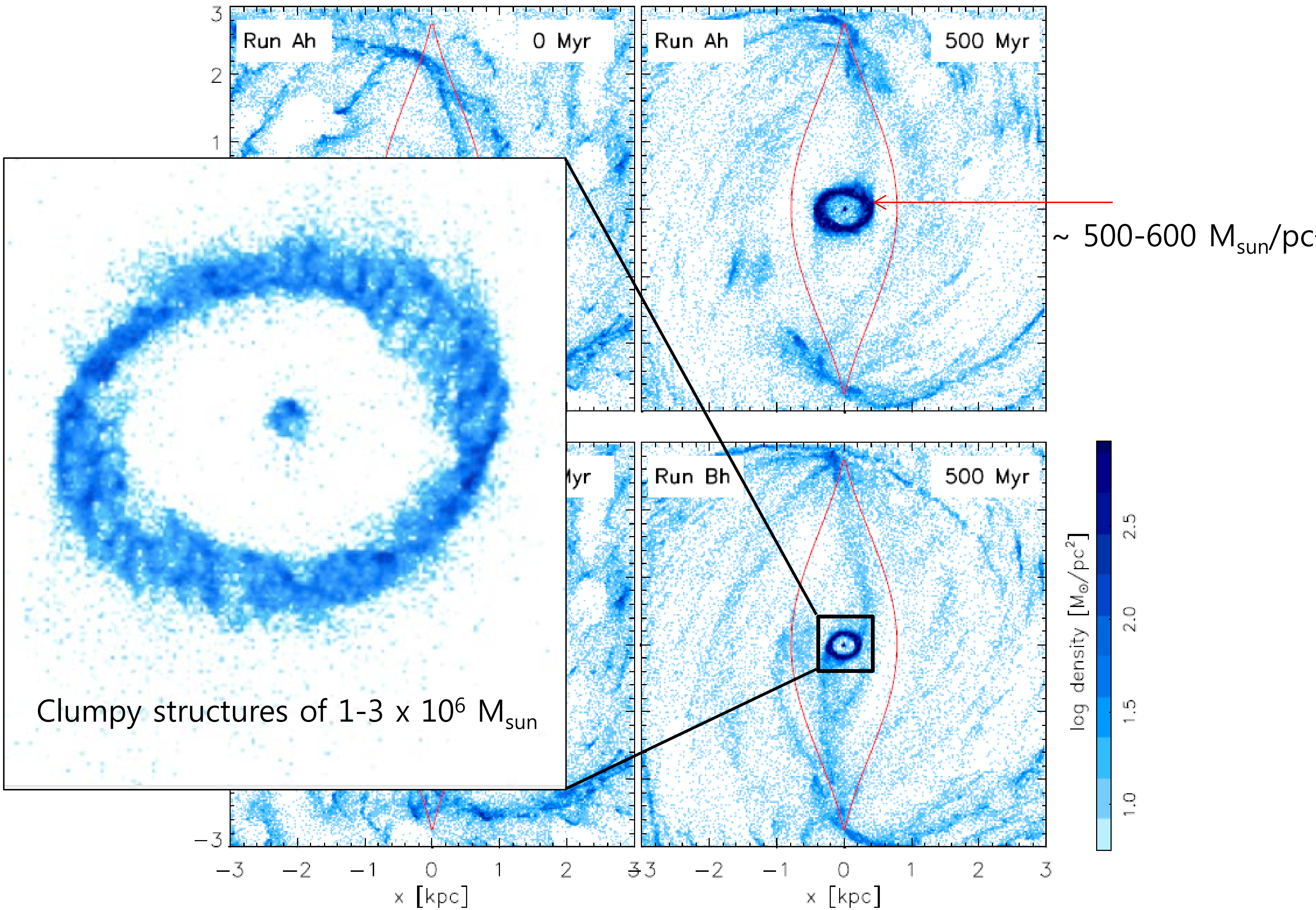

Overall morphology

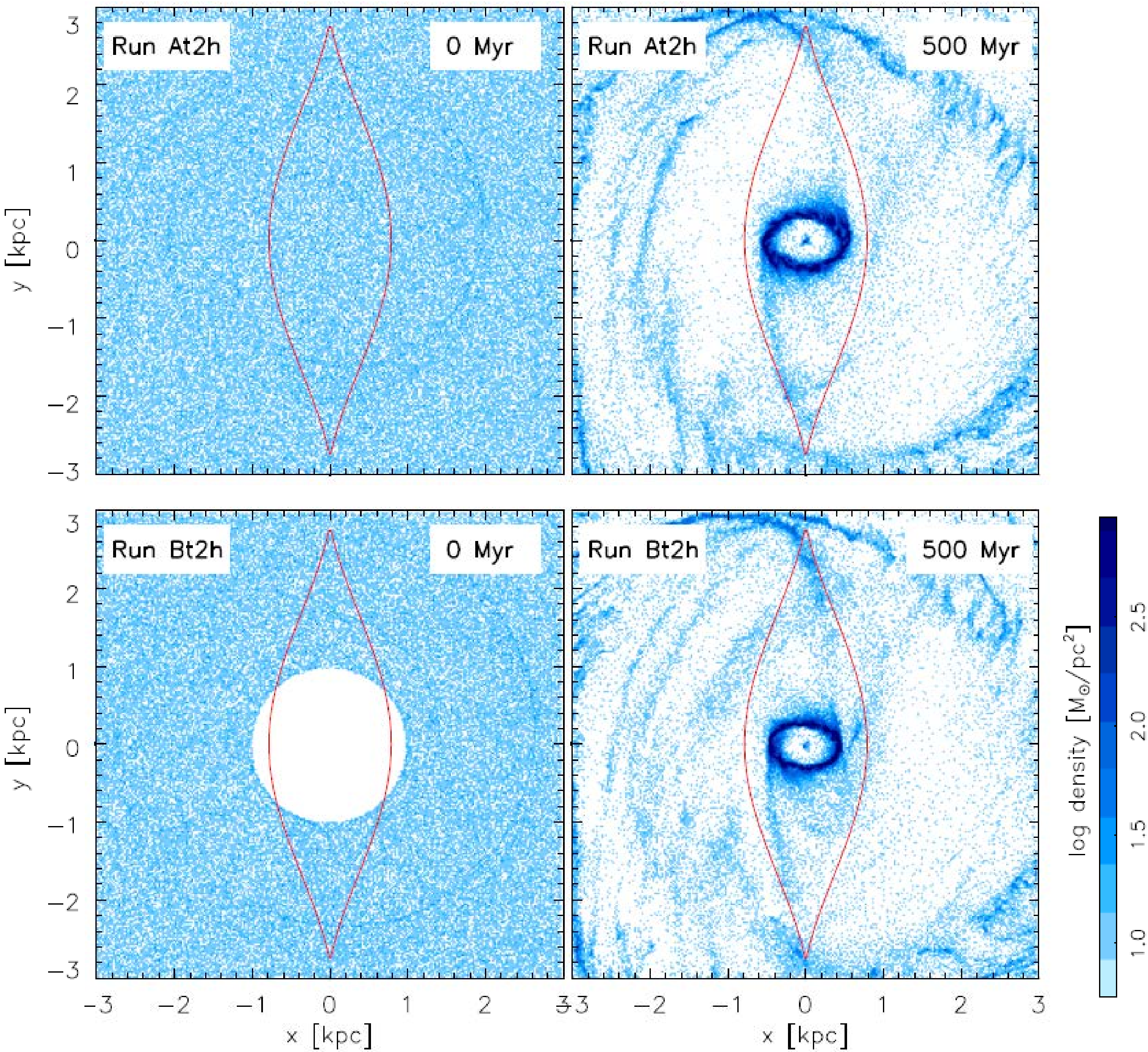

Size evolution the CMZ

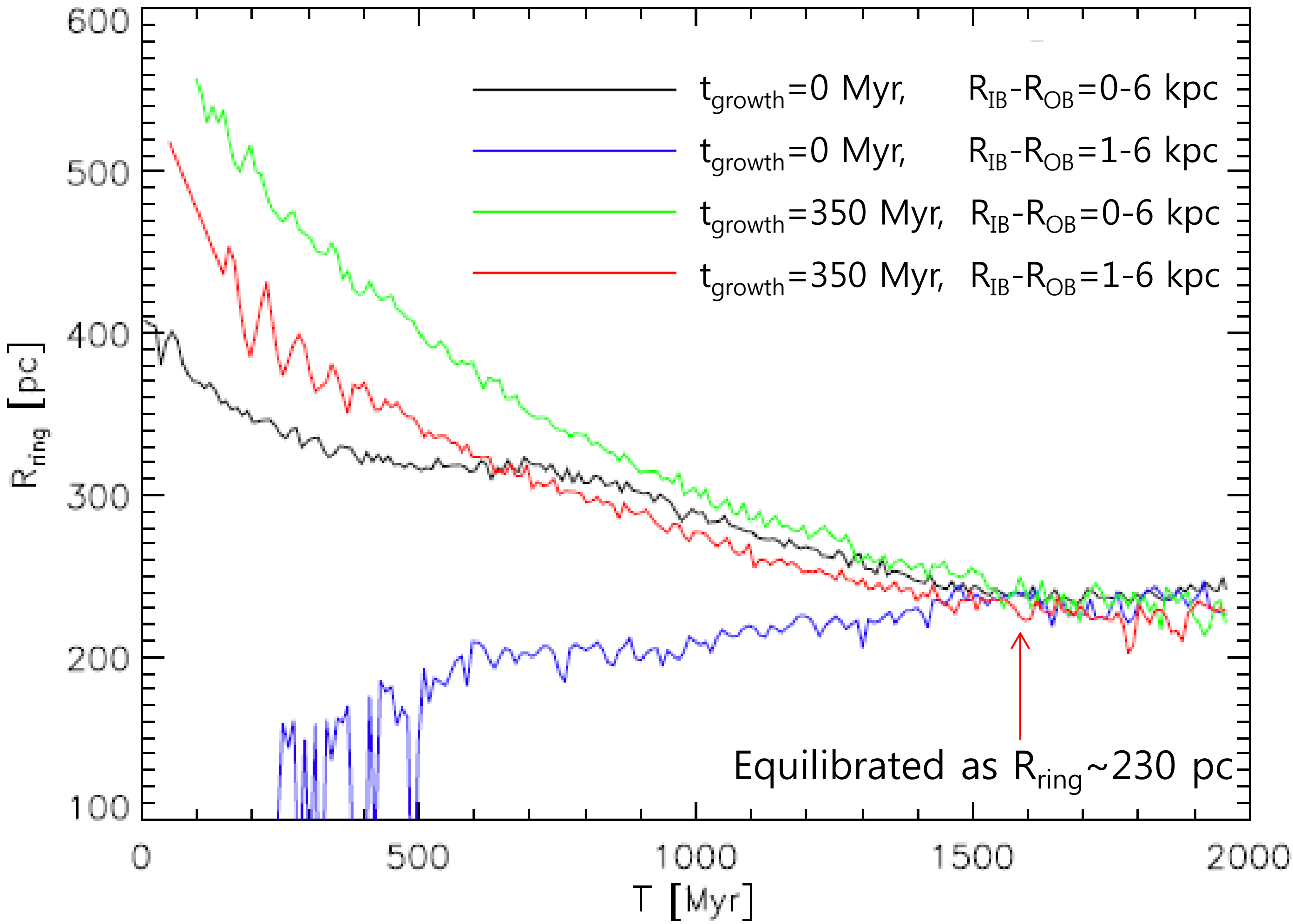

Regardless of the initial value,

all R_{ring} converge to the same value as ~230 pc at T~1500Myr.

=> a bit larger than the outer boundary of the CMZ, ~200pc (Morris & Serabyn 1996)

Gas inflows to the CMZ

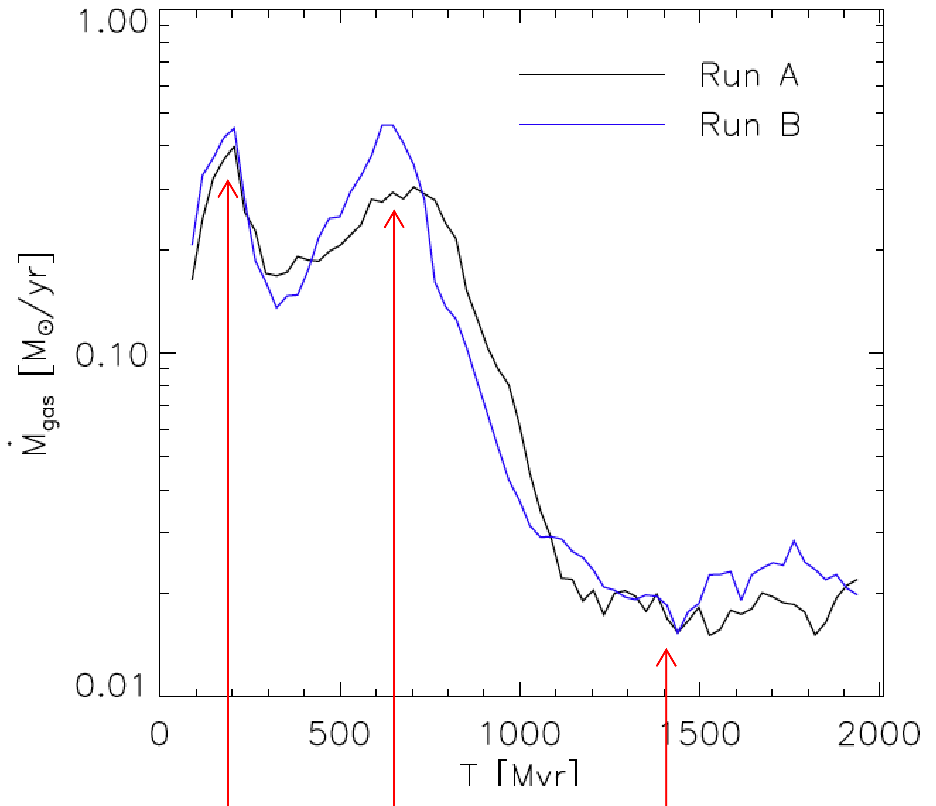

Equilibrated as ~ 0.02 M_{sun}/yr

Enhanced again by spiral shocks (Kim & Kim 2014, Seo & Kim 2014)

Initial relaxation period (due to unrelaxed gas clouds for the Galactic structure)

Gas inflows to the CMZ

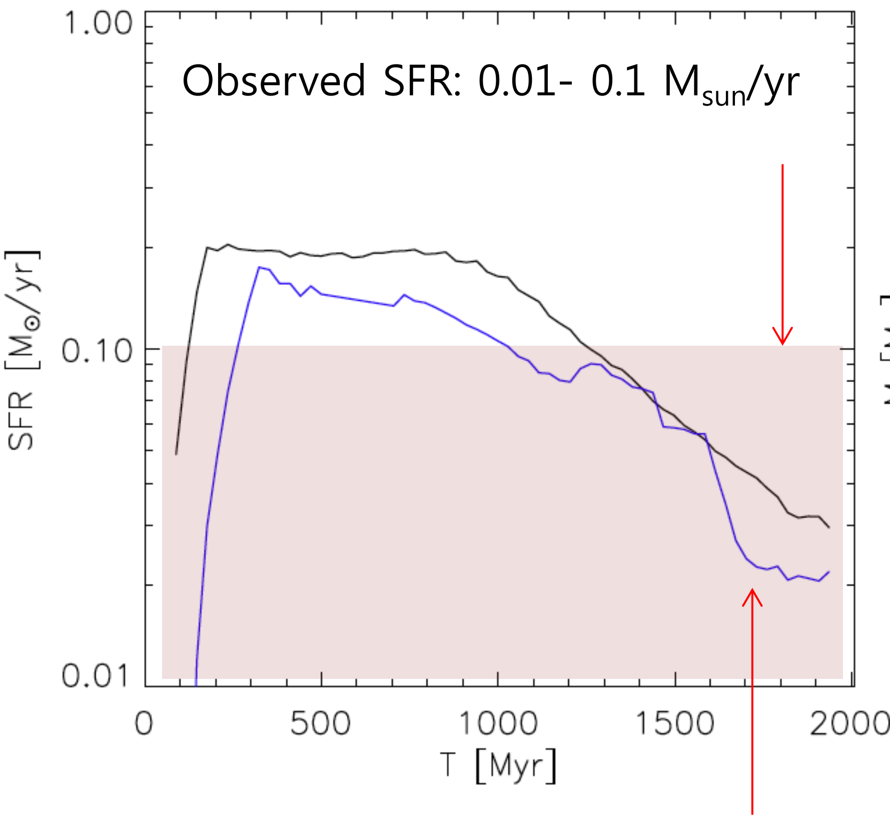

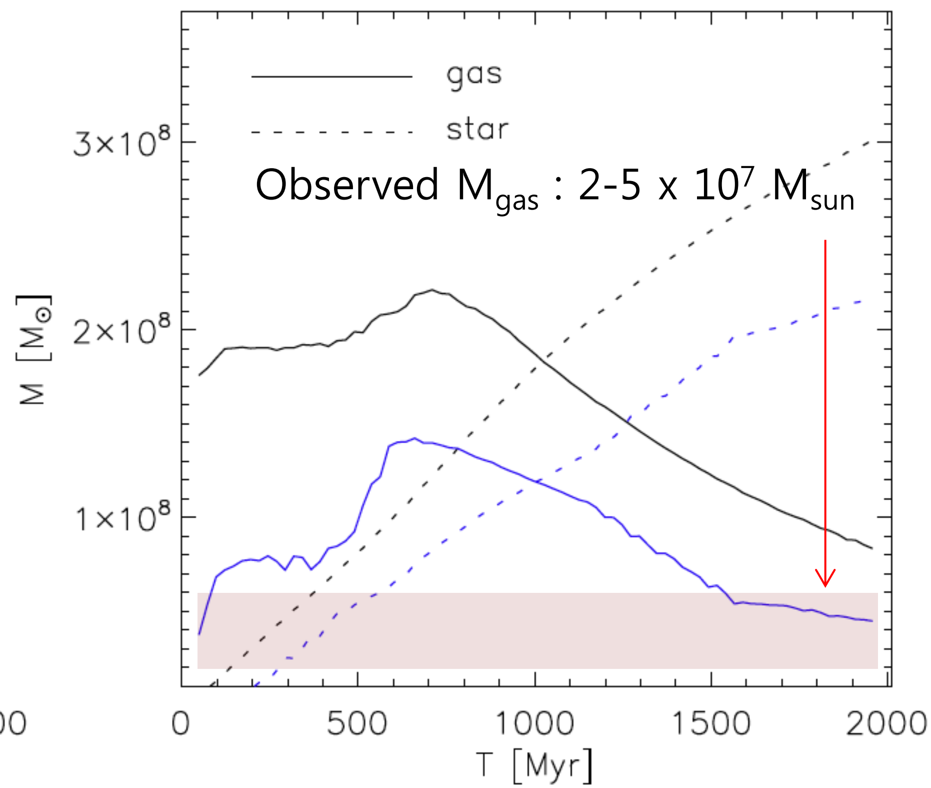

SFR is expected to be equilibrated as ~$0.02 M_{sun}$/yr

Regardless of t_{growth} and R_{IB}-R_{OB},

$\dot{M}_{gas}$, SFR and M_{gas} converge to similar ranges.

Asymmetry of the CMZ

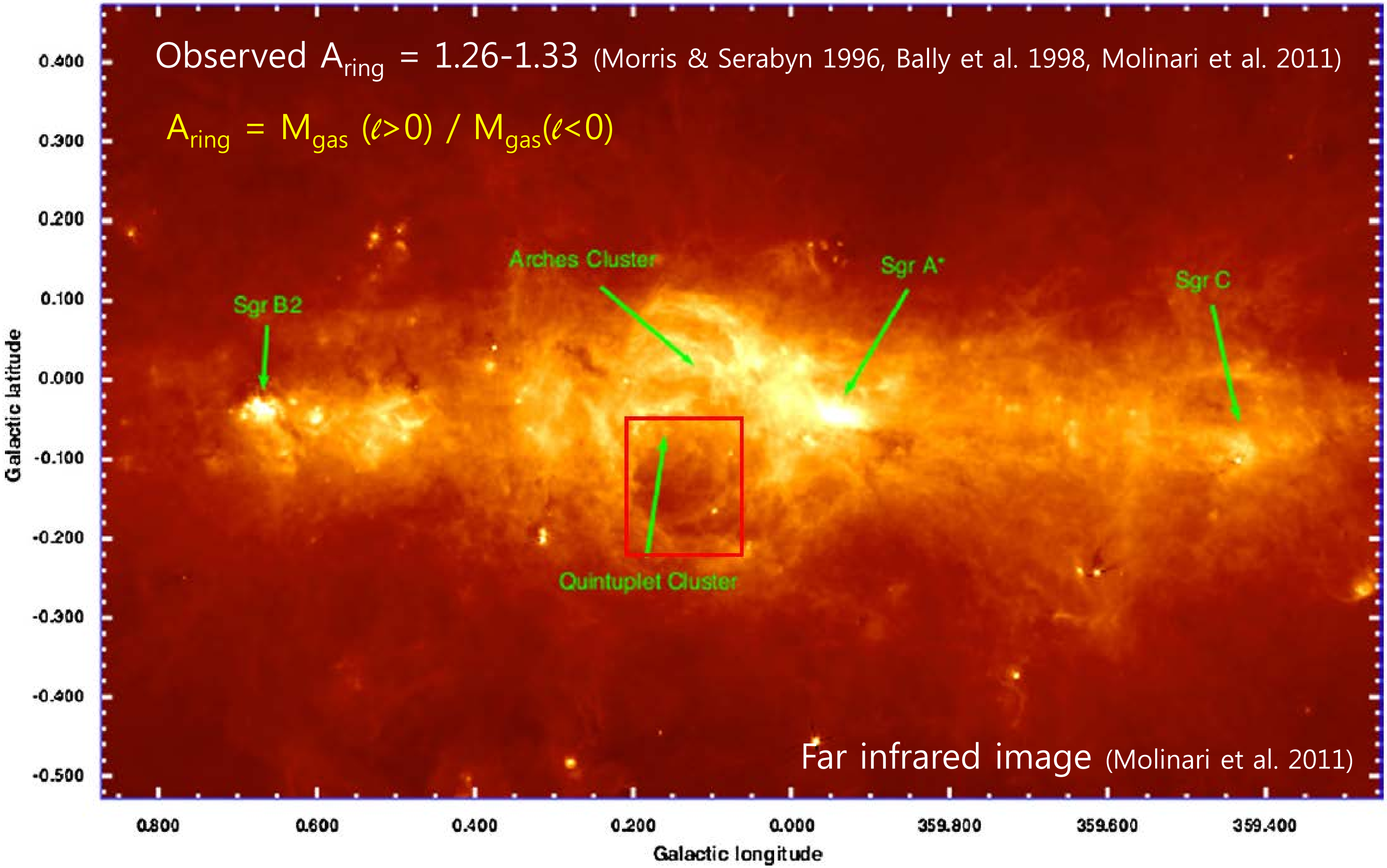

The Galactic structures of Baba (2015) -> a lopsided central mass distribution

-> an off-centered density peak of central mass distribution to the galactic center

Asymmetry of the CMZ

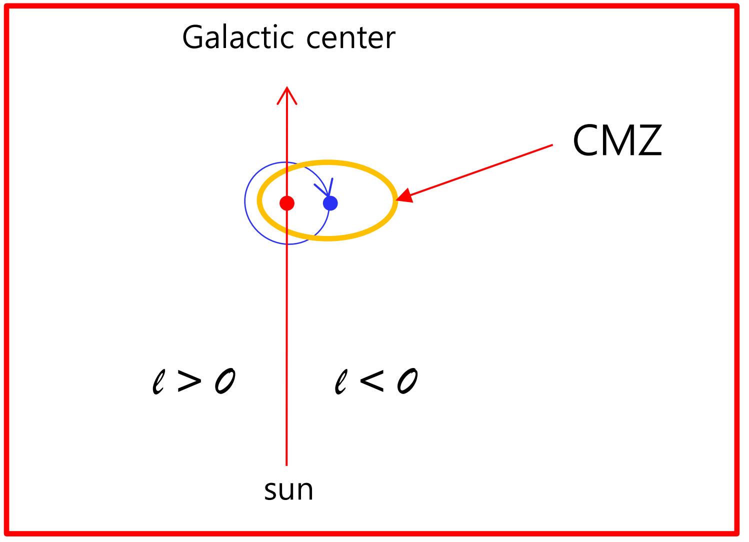

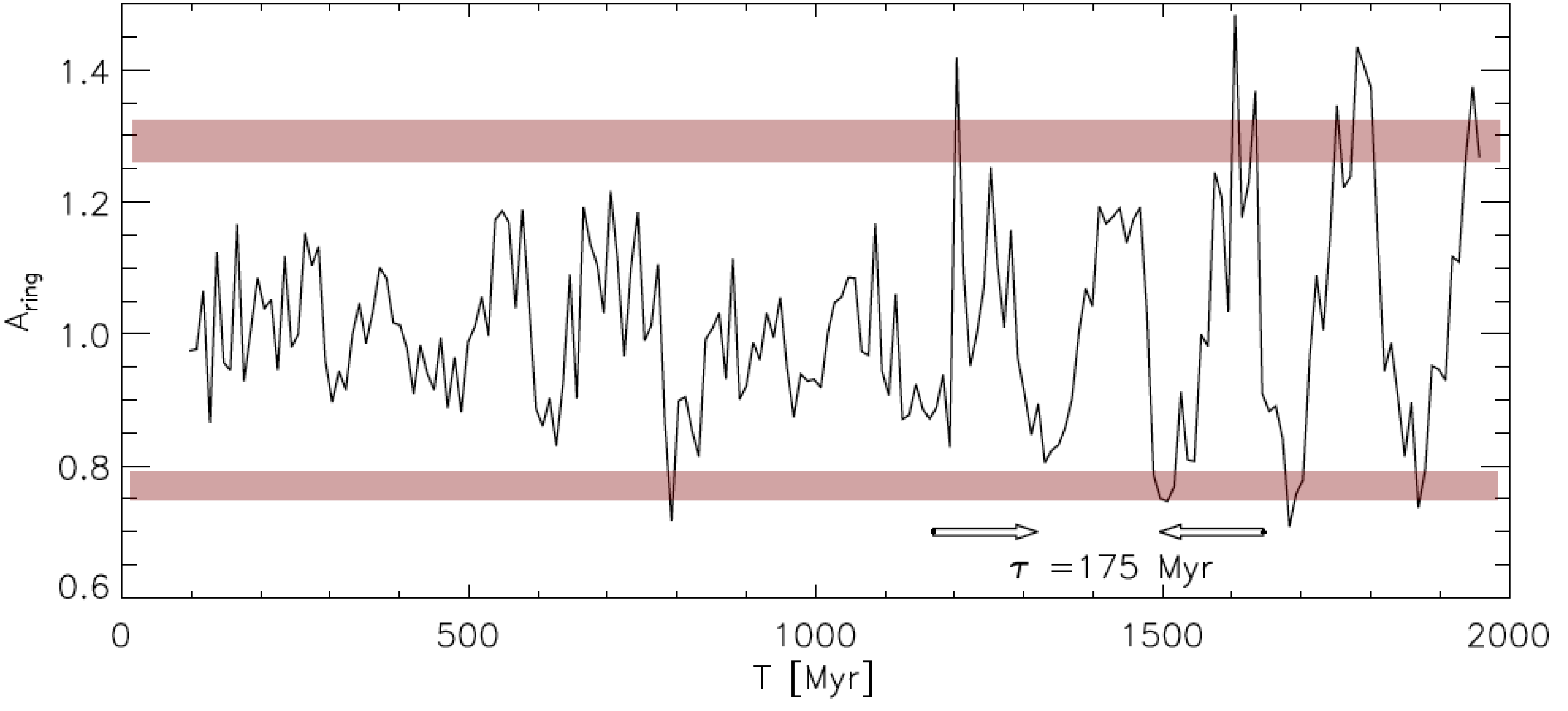

Twisted (∞-like) shape of the CMZ

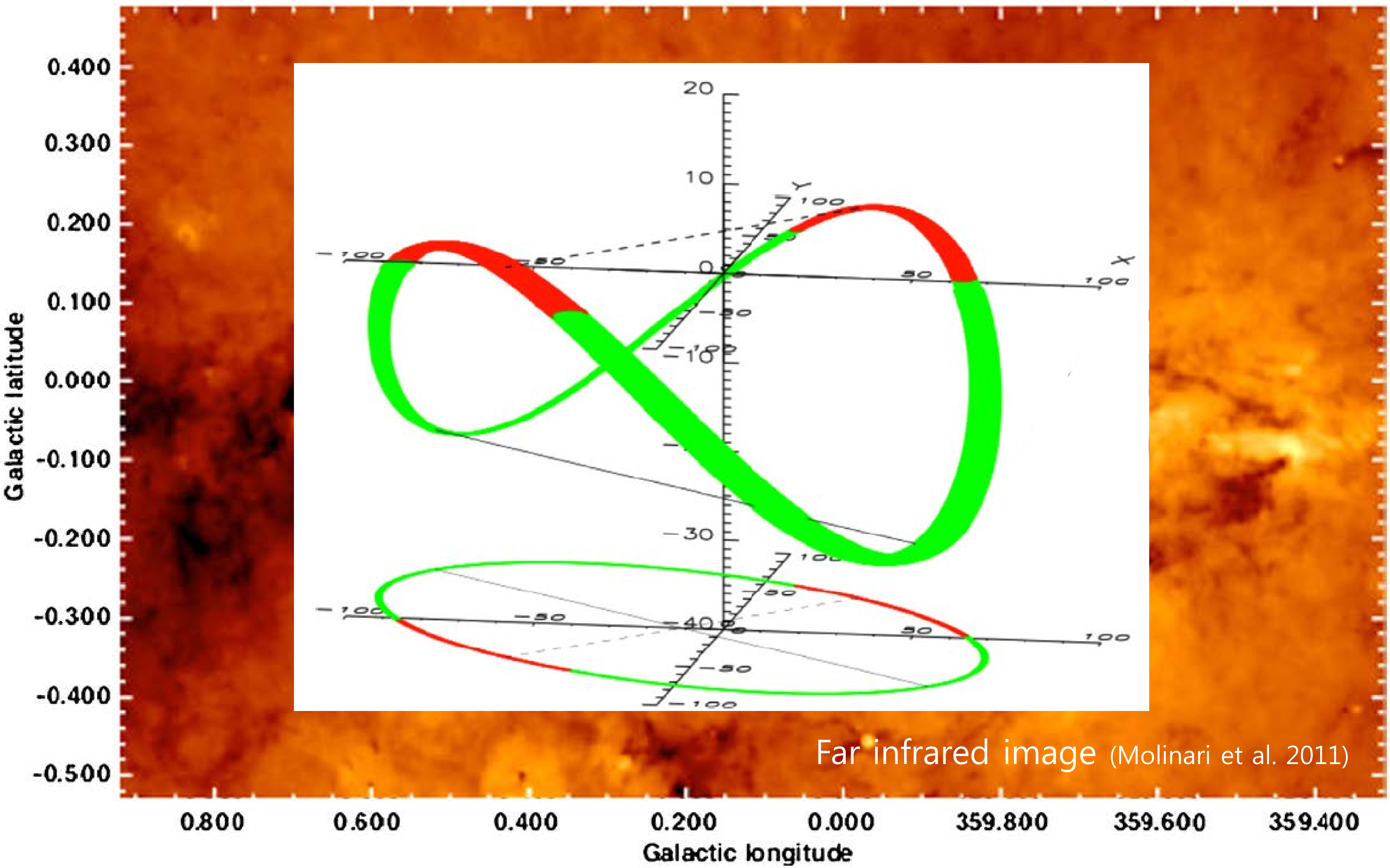

A z-directional lopsidedness of the central mass distribution -> z-directional motion

Twisted (infinity-like) shape of the CMZ

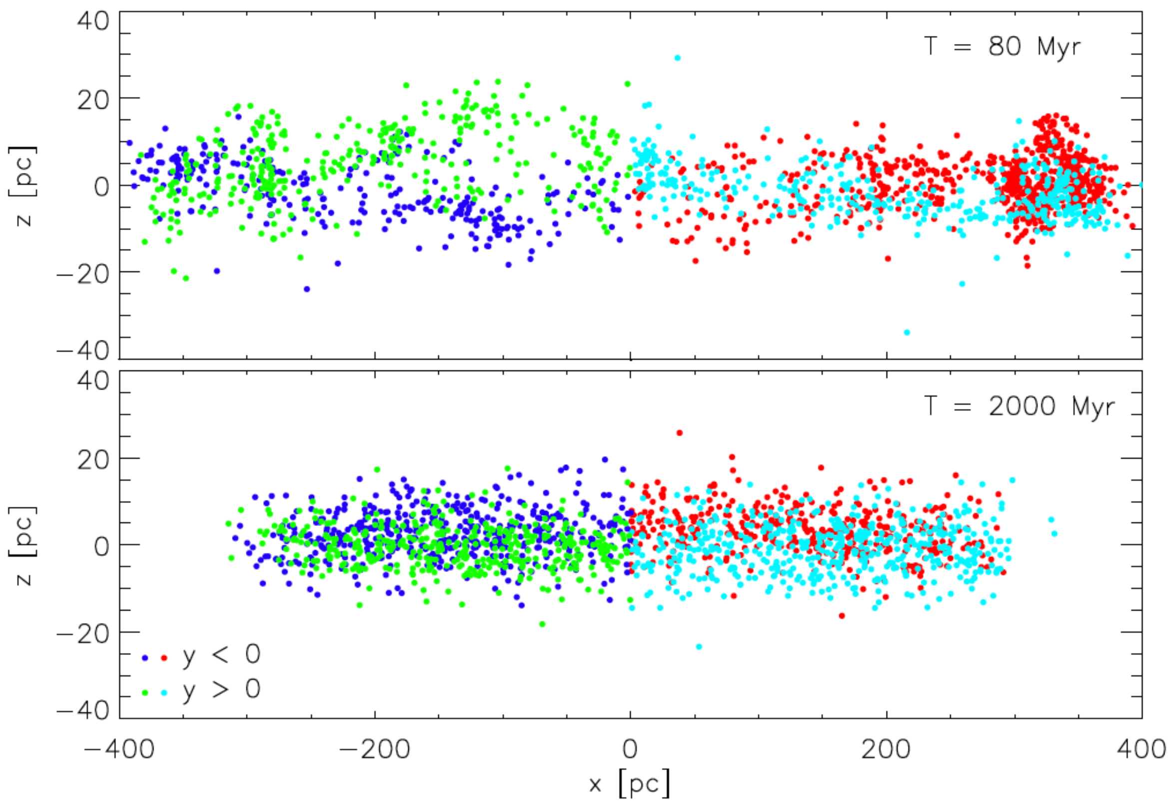

Sinusoidal shape : oscillations are synchronized to have the same phase and frequency to each other.

First 100 Myr : the z-directional frequency = 2 times of an orbital frequency -> Infinity-like shape

After the first 100 Myr : the z-directional frequency = an orbital frequency -> Tilted to the Galactic plane

Thus, the infinity-like shapes of the CMZ is dynamically young feature.

CMZ is dynamically young?

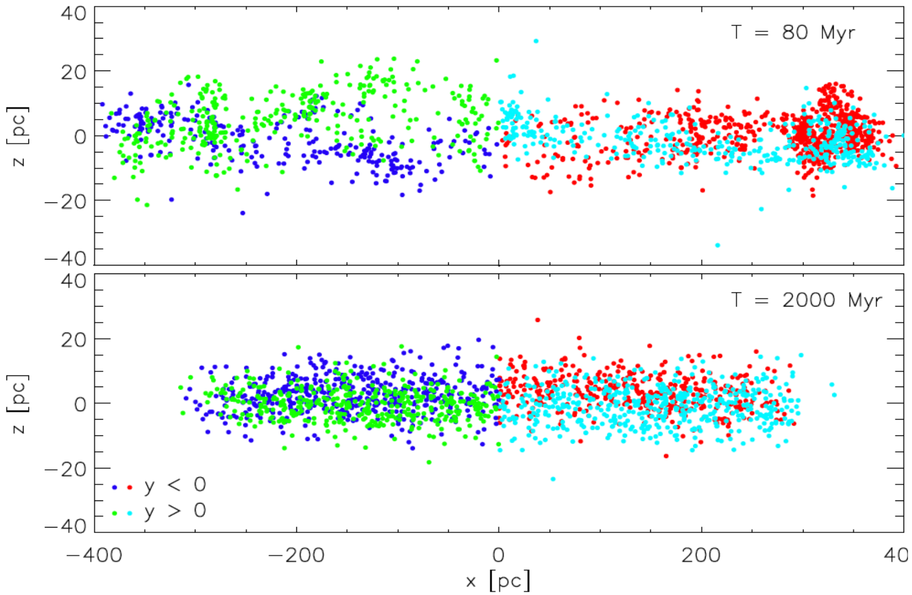

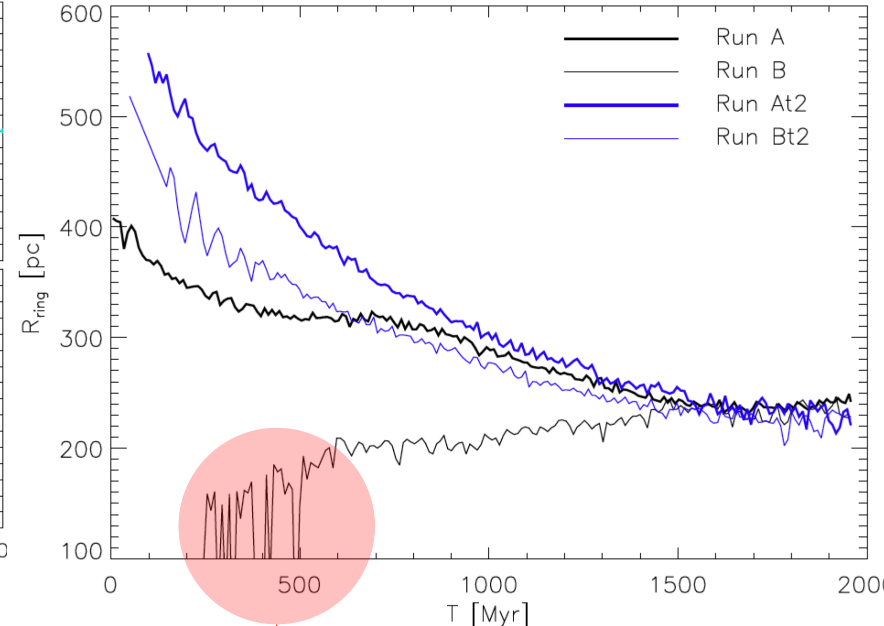

Tilted HI disk

The compact size of the CMZ is only reproduce when

- nuclear gaseous structure is dispersed by something,
- but, gas inflow from the disk is enhanced by something.

We infer that the "something" might be a minor merging event.

Summary

The ME method was utilized to efficiently include the realistic Galactic mass distribution.

: accurate and fast

: bar strength can be easily enlarged/diminished by modifying ME coefficients.

We trace the realistic motion of gas clouds from ~3kpc to ~200pc.

: R_{ring} is equilibrated as ~230 pc (most approach to the current CMZ size)

: observed M_{gas}, SFR and M_{gas} of the CMZ is well reproduced

: the lopsided central mass distribution results in

t he asymmetric mass distribution and also infinity-like feature of the CMZ.

On-going projects related with this work

: how a minor merging/fly-by disperses the nuclear gaseous structure,

and perturbs the gaseous disk (by Jihye Shin & Jeongsun Hwang)

: effect of gas replenishment to the nuclear ring (by Jihye Shin & Kyungwon Chun)

: Gas migration from CMZ to CND (by Hannah Morgan, KHU)

: tilted HI disk (by Joowon Lee)

: bar strength of external barred galaxies using ME method (by Eunbin Kim)